DET NORSKE VIDENSKAPS-AKADEMI I OSLO

GEOFYSISKE PUBLIKASJONER
GEOPHYSICA NORVEGICA

Vol. XXVI. No. 5 February 1966

JACK NORDÖ

The Vertical Structure of the Atmosphere

OSLO 1966
UNIVERSITETSFORLAGET

GEOFYSISKE PUBLIKASJONER
GEOPHYSICA NORVEGICA
VOL. XXVI. NO. 5

THE VERTICAL STRUCTURE OF THE ATMOSPHERE

By Jack Nordø

FREMLAGT I VIDENSKAPS-AKADEMIETS MØTE DEN 22. OKTOBER 1965 AV FJØRTOFT

Abstract. Optimal parametric representations of atmospheric temperature and wind distributions are derived. As parameters are used heights of prescribed pressure surfaces. The reliability of the empirical relations are demonstrated by empirical measures of dispersion. Some applications to the problem of designing atmospheric models are suggested.

1. Introduction. The research reported in this paper was partly carried out when the author worked at the University of Oslo, 1950—55*. Some of the main results were discussed in lectures presented at the Norwegian Meteorological Institute and at the University of Bergen. Obukhov (1960) has carried out similar investigations, using empirical orthogonal functions. Holmström (1963, 1964) has lately published some interesting investigations also using orthogonal functions in describing the vertical distribution of variables.

Our investigation was inspired by the papers on quasi-geostrophic 1—4 layer models published in the early 1950's, see e.g., A. Eliassen (1952), Charney and Phillips (1953). But the results should also be useful for the primitive equations approach. In this period the typical computer speed was much less than at present, and it became very mandatory to optimize the models. One obvious approach would be to select those levels which give maximum information about the vertical structure of the atmosphere, and this became the aim of our investigation. The perfection of, and increased speed of, recent computers have stimulated bolder approaches, as e.g. that of Smagorinsky and his group (1965). He is reporting success with a 9-layer model.

But it is a general experience that a multi-level model requires a very good, and *consistent* analysis to minimize aliasing effects. At present a WMO committee (1965) is planning another international move to increase the number of weather observations in sparsely populated regions, using a.o. satellites to receive and distribute the data. It is not likely however, that we will have considerable improvements in the near future.

Besides the modelling uses of the vertical structure of the atmosphere, such interrelations of temperature, wind and height might be very important in numerical ana-

* Sponsoring agency: Norges Almenvitenskapelige Forskningsråd.

lysis when checking the data, replacing missing data by interpolation, and specifying prognostic maps at levels different from those used in the operational models.

The best data available in the early fifties were the punchcards of the upper air data from the United Kingdom stations and the two English weatherships in the Eastern Atlantic Ocean. Wind, temperature and geopotential heights were observed every six hours of the day. The following study is based on data from the months of October 1950 through March 1951, and October 1951 through March 1952. As the stations JIG JULIETTE (52½° N, 20° W), LERWICK (60°08′ N, 01° 11′ W) and DOWNHAM MARKET (52°37′ N, 00°24′ E) appeared to have the most reliable records, we shall normally use these three stations to demonstrate our results. To avoid most of the effects due to seasonal trend in the data, correlations were computed for each month. Then we used the Fischer z-transformation, $z=\frac{1}{2}\ln(1+r)/(1-r)$, converting the coefficient of correlation r to a normally distributed quantity. Average values of z were established for various interrelations. The temperature of the 1000 mb-level will be put equal to the surface temperature, although this assumption may lead to a systematic bias in the Ekman layer of the atmosphere.

2. Intercorrelations of heights of isobaric levels. Let us denote the heights of the 1000 mb, 700 mb, 500 mb and 300 mb levels by H_{1000}, H_{700}, H_{500}, H_{300}, respectively. Figure 1 gives then the average intercorrelations for the records at the three reference stations. The intercorrelation curve seems to be smooth, falling off very steadily with

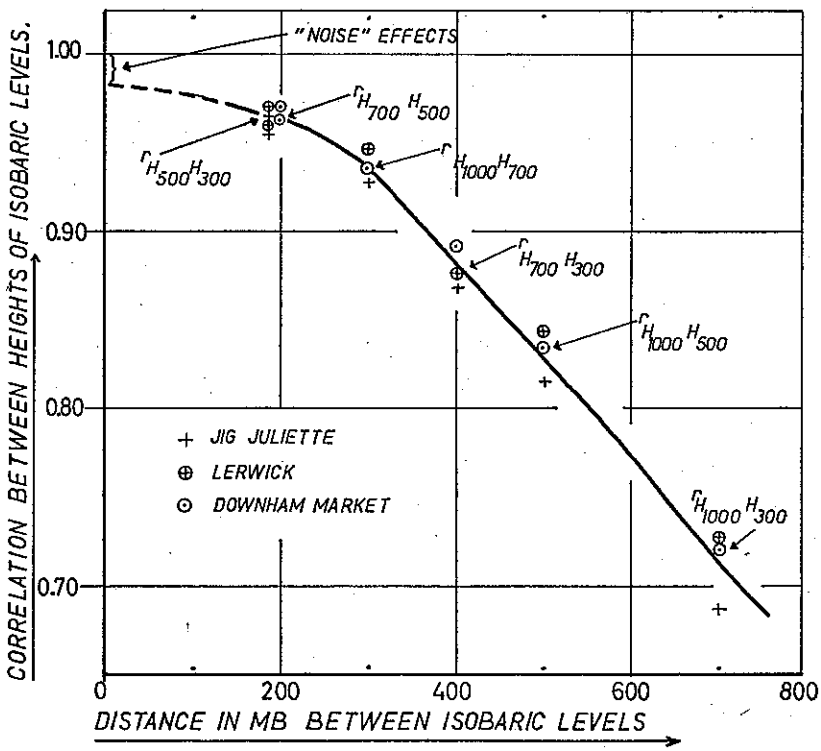

Fig. 1. Correlation between heights of isobaric levels.

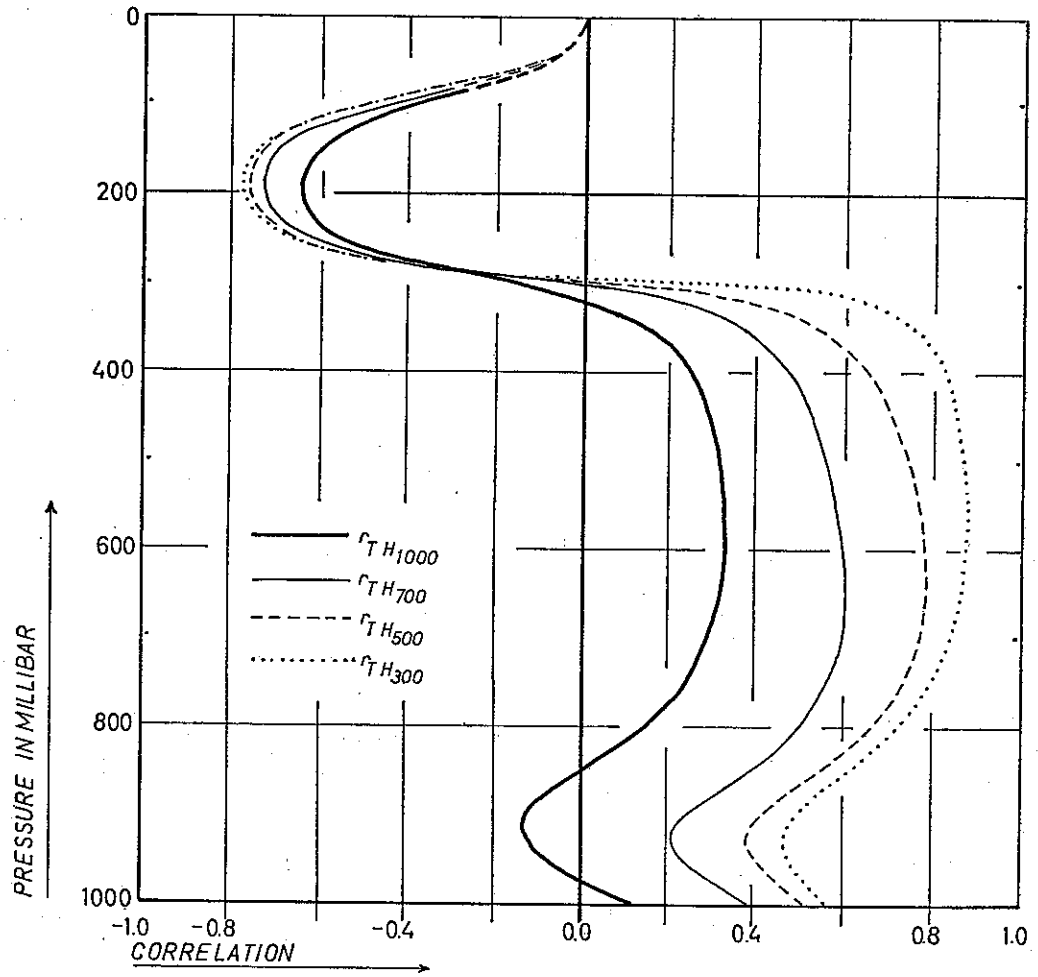

Fig. 2. Correlations of temperature (T) and height (H).

increasing pressure difference. The seasonal trend is also negligible in the two winters under consideration. This is remarkable, as the trends in the means and the variances are pronounced. The stability of the correlations are best illustrated for the interval of 200 mb. For this distance we have computed 72 sample correlations, of which 8 were above 0.98 and 11 below 0.92.

We have extrapolated the correlation curve until zero distance, suggesting a value less than 1.00. The reason for this is that there is a systematic tendency of noise effects (small scale disturbances and instrumental errors) to reduce the coefficient of correlation.

Another significant information about the vertical structure of the troposphere is revealed by the partial correlations $r_{H_{300}\,H_{700}\cdot H_{500}} = -0.607$ and $r_{H_{300}\,H_{1000}\cdot H_{500}} = -0.606$, which are the correlations we obtain between H_{300} and H_{700} (or H_{1000}), when the effects of their correlations to H_{500} are eliminated. The negative values of the partial correlations are caused by baroclinic and frontal effects, i.e., the thermal field has an overall

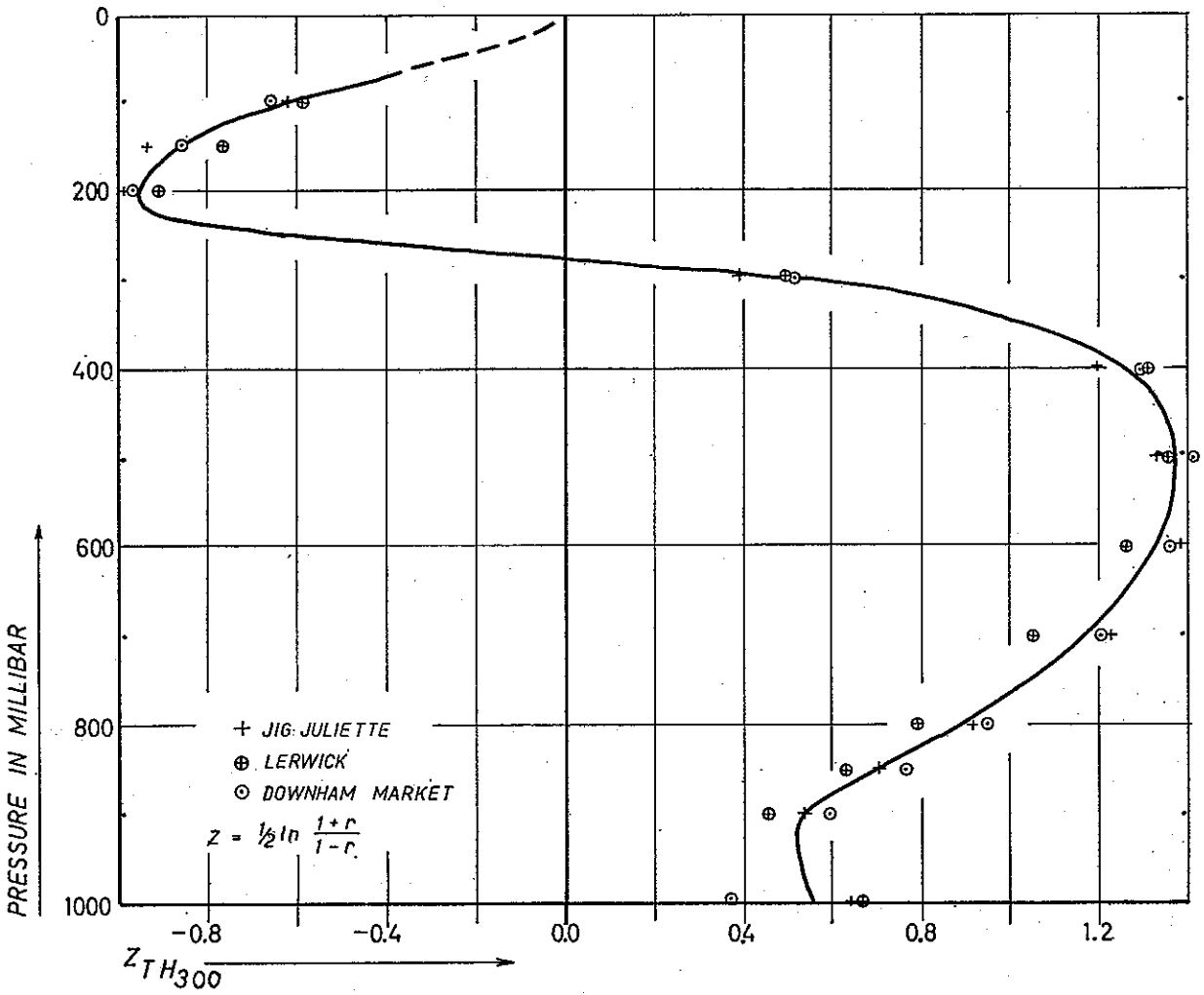

Fig. 3. z-transformed correlations of temperature and H_{300}.

tendency to be out of phase with the 500 mb heightfield. The stability of the negative partial correlations is given by the following frequency distribution, comprizing 72 monthly sample values.

Table 1. *Frequency distribution for* $r_{H_{300}\, H_{700}\, .\, H_{500}}$ *and* $r_{H_{300}\, H_{1000}\, .\, H_{500}}$

Interval	−0.84→−0.75	−0.74→−0.65	−0.64→−0.55	−0.54→−0.45	−0.44→0.00
Frequency	7	19	19	18	9

The correlation between H_{300} and H_{1000} for given values of H_{500} and H_{700} is given by the partial correlation $r_{H_{300}\, H_{1000}\, .\, H_{500} H_{700}} = -0.196$. This is the mean value, out of 36 sample values we find 3 cases beyond -0.40 and 5 positive cases. If we compare with the value of $r_{H_{300} H_{1000}\, .\, H_{500}}$, we realize that an essential part of the "frontal" effects is taken care of by H_{700}.

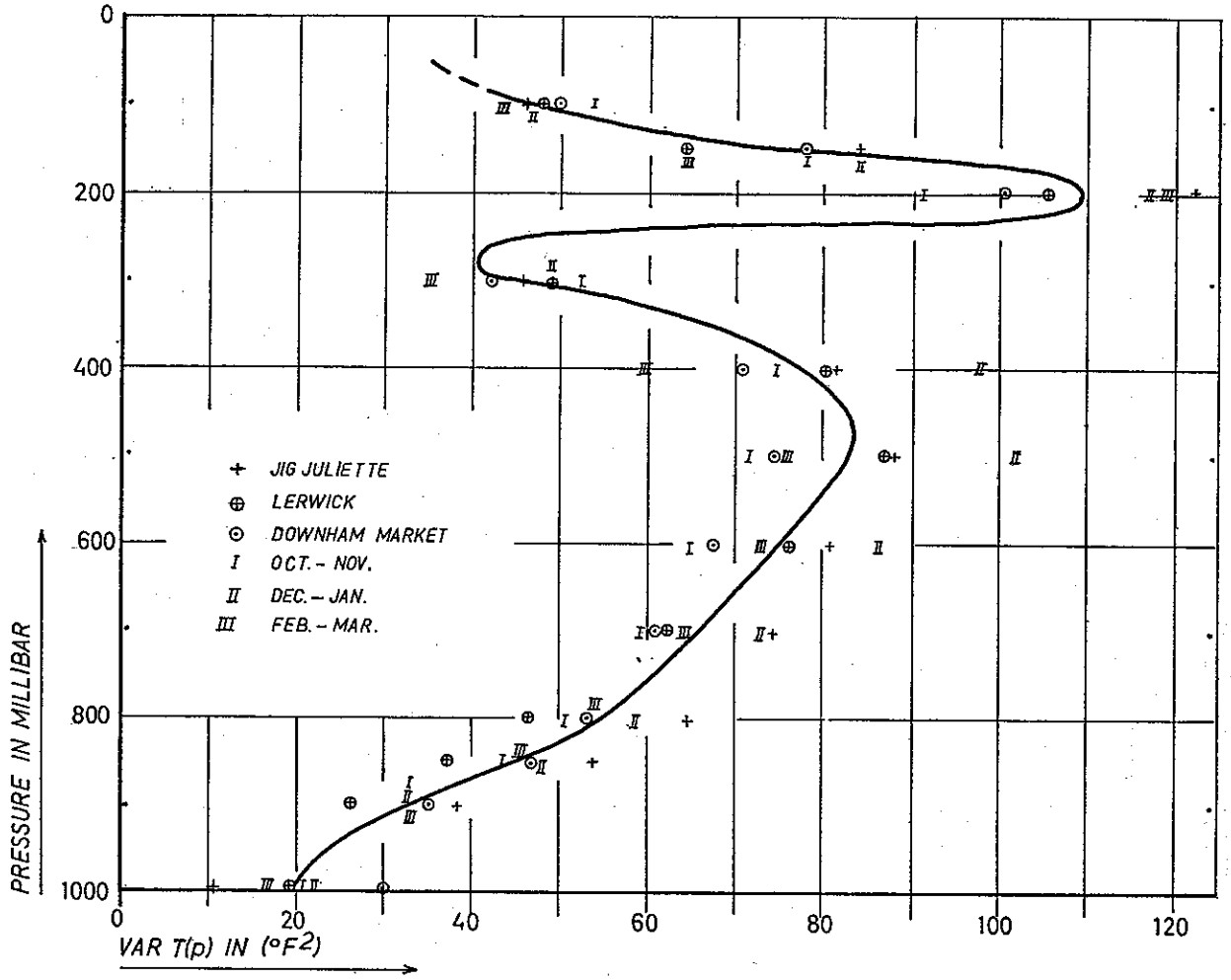

Fig. 4. Vertical distribution of the variance of temperature.

3. Correlations between the vertical temperature distribution and the height of a given isobaric level. For every 100 mb level from 1000 mb to 100 mb, including 850 mb and 150 mb, we have correlated the temperature with the height of a prescribed pressure level. The first interesting results are given in Fig. 2. The ordinate is pressure in mb, and the abscissa is in the common units for the correlation coefficient, which is non-dimensional.

We notice that the height of the 300 mb level gives the best estimates of the temperature throughout the complete troposphere. The geographic stability of this relation is best illustrated in Fig. 3, where the z-transformed correlations between height of 300 mb (H_{300}) and the temperature $T(p)$ are given for the three reference stations cited above. The variability is fairly small, and this fact suggests that our results should be representative for the whole Eastern Atlantic region. It is noticeable that the correlation for surface temperature is low for DOWNHAM MARKET. This reflects some continentality, as the surface temperature of the northern continents is almost independent of H_{500} (or H_{300}) in the winter season. Figure 3 reveals the significance of the old synoptic rule that if H_{300} is high, the troposphere is warm and the stratosphere is cold (subtropical

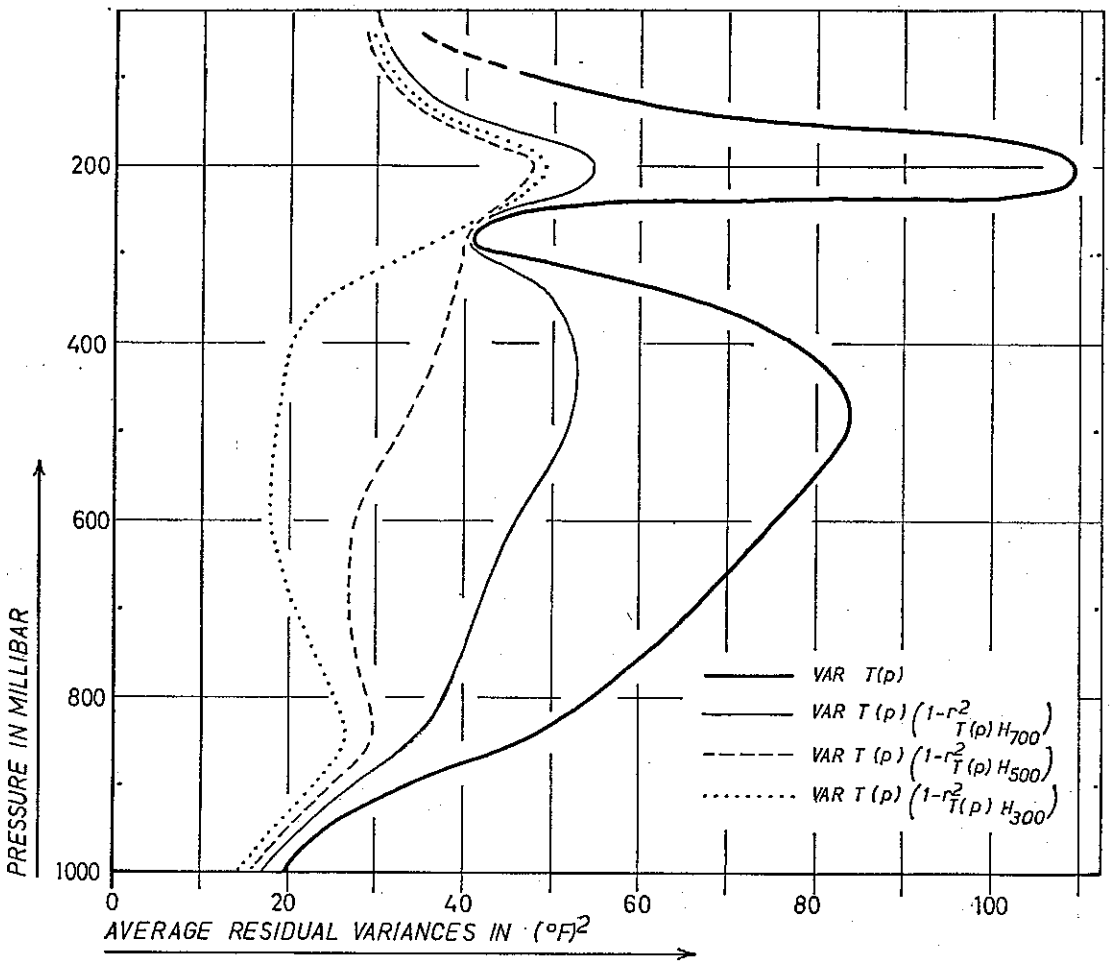

Fig. 5. Vertical distribution of temperature residual variances.

air mass). Vice versa, a low value of H_{300} tends to be accompanied by a cold troposphere and a warm stratosphere (polar air mass).

Let var $T(p)$ denote the sample variance of temperature at the pressure level p. The residual variance, var $T(p)\{1-r_{T^2(p)H}\}$, is a measure of the uncertainty in determining the vertical temperature distribution by the height of one isobaric level only. But var $T(p)$ has definitely both a geographic variation and an annual variation, and the data from the two winters cannot give us a good estimate of the population variances. However, some of the basic features of the vertical variability of temperature should show up in our study. Figure 4 reveals our results in condensed form. The peaks at about 500 mb and 200 mb are very pronounced, and may be related to the vertical velocity variations in connection with waves on synoptic scales. In 28 out of 36 cases, the stratospheric maximum was predominant. But as the static stability of the stratosphere is very high, a minor displacement there may cause the same temperature variation as a major vertical displacement in the troposphere. The minimum close to 275 mb is very pronounced.

We did not have any reliable data beyond 100 mb, but other extremes may be ex-

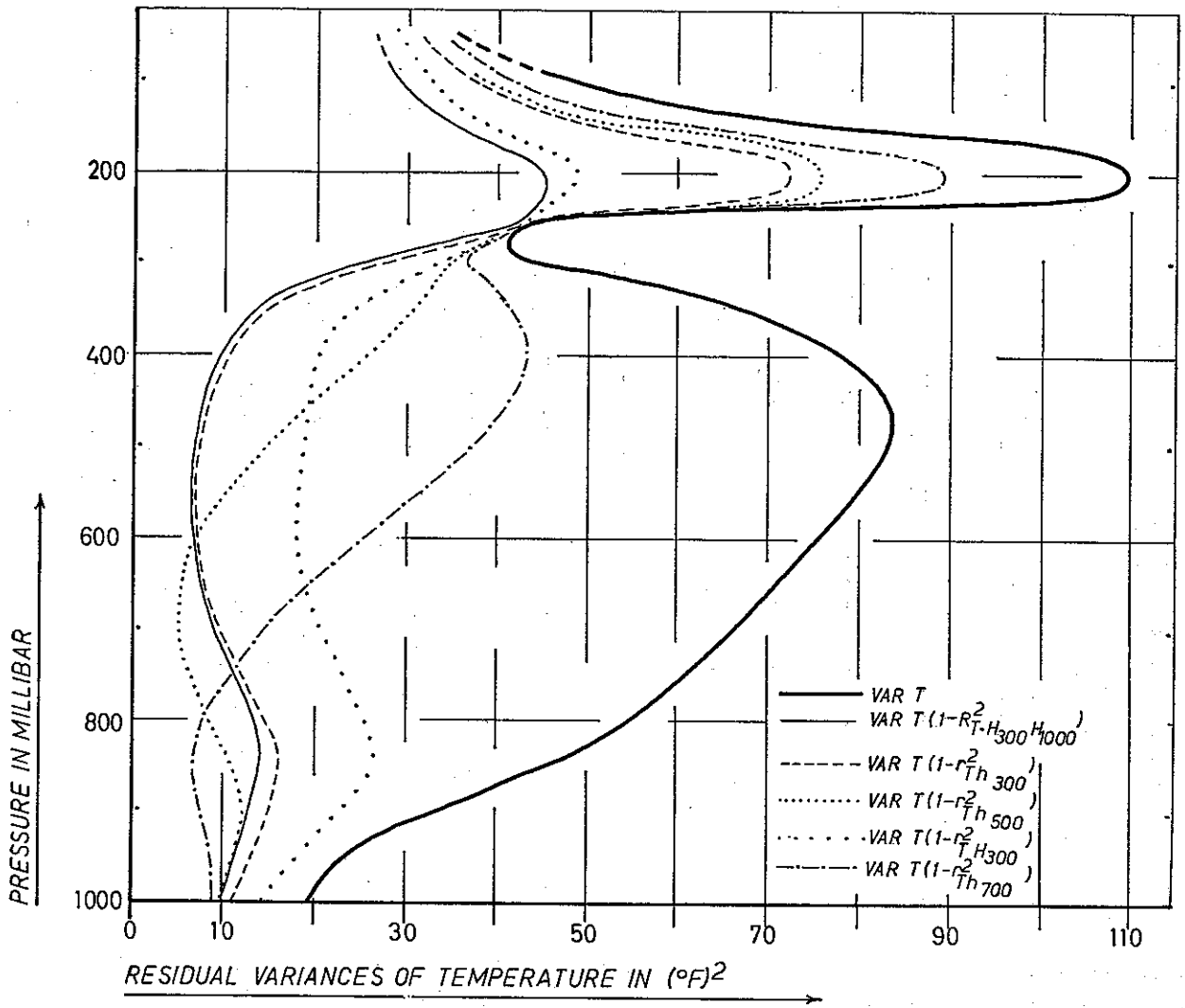

Fig. 6. Residual variances when $T(p)$ is correlated to tropospheric thicknesses.

pected. We should also notice that the seasonal trend is rather pronounced in the upper troposphere where the December-January average variances are running close to 100 (°F)².

The average values of the residual temperature variances are shown in Fig. 5. We notice once again that H_{300} is significantly better than H_{500} when specifying tropospheric temperature distributions. Moreover, investigating 252 sample residual variances of temperature at the pressure levels from 850 mb to 300 mb, only seven cases (4 at 300 mb, 2 at 800 mb and 1 at 850 mb) were in favour of using H_{500} rather than H_{300} in specifying the temperature.

4. Vertical temperature distributions specified by a tropospheric thickness. Next we shall consider the correlations of the temperatures and the thickness, h, between a given pressure level and the 1000 mb level i.e., $h_{700}=H_{700}-H_{1000}$, $h_{500}=H_{500}-H_{1000}$,

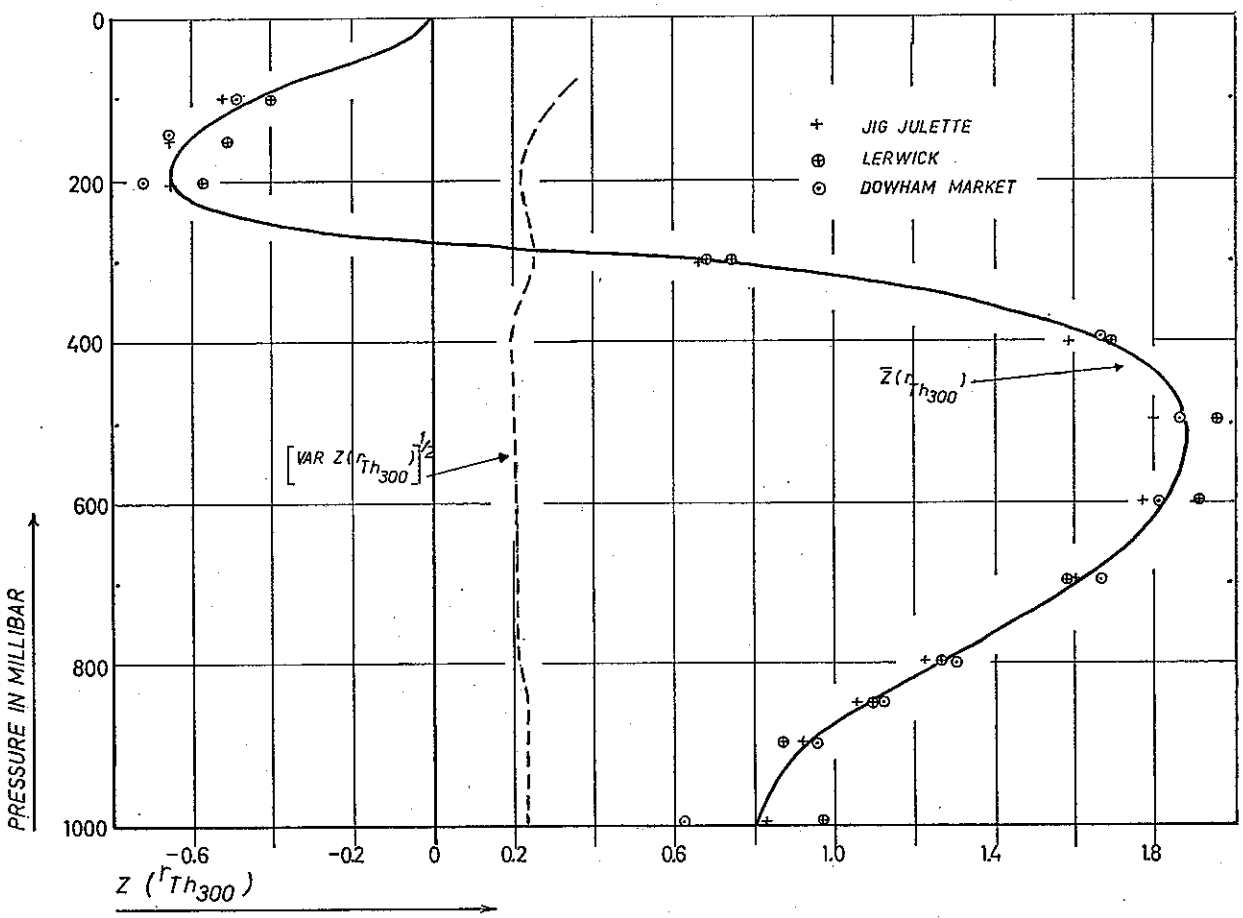

Fig. 7. Correlations of temperature and thickness at three stations.

and $h_{300}=H_{300}-H_{1000}$. The means of all 36 monthly residual variances at the three reference stations are shown in Fig. 6. We shall also give the corresponding curves when temperature is related to H_{300} only, and to H_{300} and H_{1000} simultaneously by multiple regression. First of all we shall notice that H_{300} describes the stratosphere temperatures better than any of the three thicknesses. Further on, H_{300} is better than h_{500} when specifying the temperature at levels above 500 mb. This is indeed a very remarkable finding, as h_{500} is the thickness preferred in most 2-level models of the atmosphere. The residual variance is fairly low throughout the troposphere when the temperatures are specified by h_{300} or the multi-regression scheme of H_{1000} and H_{300}. But the latter set of variables is superior for the lower stratosphere. Figure 6 shows also the following anticipated features:

1. h_{700} takes good care of temperature variations at the levels below 750 mb.
2. h_{500} describes well the temperature variations between 600 mb and 1000 mb.
3. None of the tropospheric thicknesses used above, give any good estimate of the stratospheric temperature distribution.

The stability of some of the best relations are shown by the following frequency distributions of the sample residual variances of $T(500)$ and $T(600)$.

Table 2. *Frequency distribution of residual variances in* $(°F)^2$.

	Residual Variances								
	0→2	2→4	4→6	6→8	8→10	10→12	12→14	14→20	20→35
Using H_{300}	0	0	3	2	3	6	5	27	26
Using h_{300}	0	8	14	27	11	8	4	0	0
Using H_{300}, H_{1000}	0	9	22	27	7	5	2	0	0

If we use e.g. the H_{300}, H_{1000} system, 65 out of 72 cases have a residual variance less than 10 $(°F)^2$ or $(1.75\ °C)^2$, which is a rather promising result.

The geographical stability of $r_{T(p)h_{300}}$ is displayed by its z-transformed values in Fig. 7. The partial correlation $r_{TH_{1000}.H_{300}}$ is plotted on the same scale in Fig. 8. It is obvious that this partial correlation should be significantly negative throughout the troposphere, as a high tropospheric thickness should give a warm troposphere.

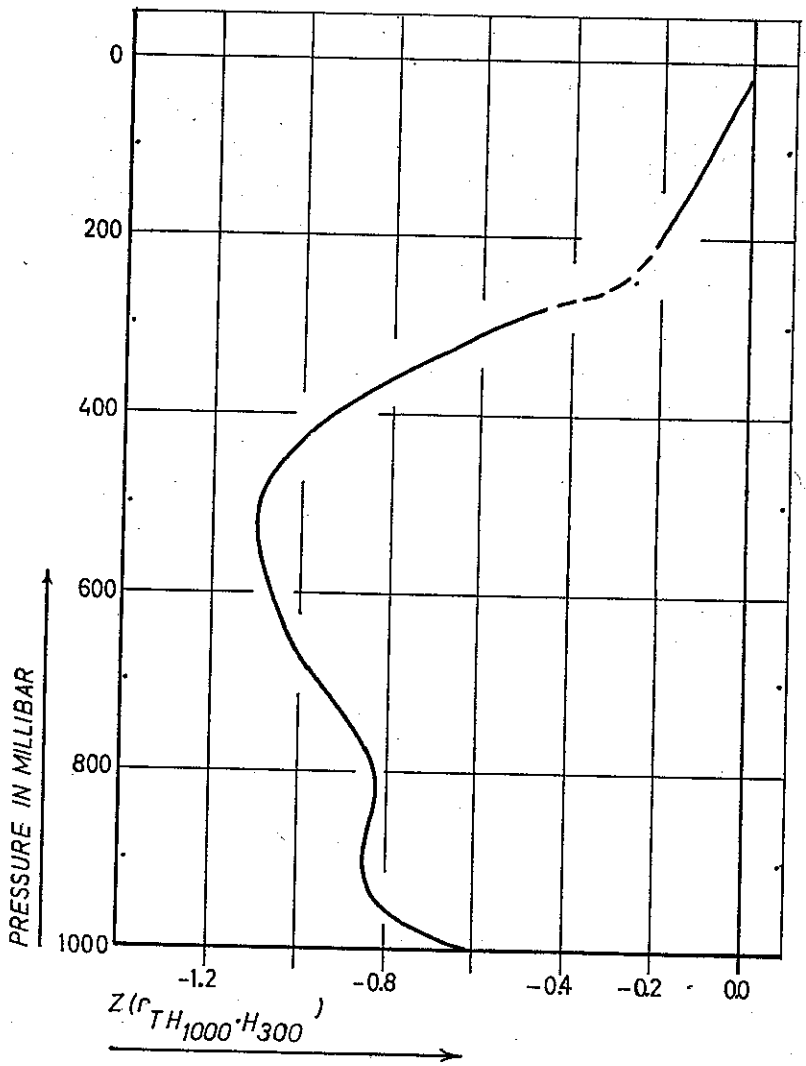

Fig. 8. Partial correlation of temperature and H_{1000}.

5. Derivations of relations for the quasi-geostrophic wind. A general discussion of quasi-geostrophic models are given by e.g. A. ELIASSEN (1952), and CHARNEY and PHILLIPS (1953). But as the non-geostrophic part of the wind is rather important, we feel that a general balanced model should be tried instead. In such models we may consider the geostrophic wind as a first approximation. The higher order approximations are computed by an iterative scheme using the geostrophic approximation as a first guess, see e.g. FJØRTOFT (1962). Most of the following discussion refers therefore to a parametric representation of the geostrophic flow. As these empirical relations may be useful in a variety of models, we have refrained from giving priority to a special version.

Applying the geostrophic approximation we can establish a relation between vertical wind-shear and the thickness, namely the thermal wind equation. But we may also approach the problem in the more general way suggested in the first part of this paper, i.e., we may try to derive by the least squares procedure a linear relation which determines the temperature at any level by the heights of certain specified isobaric levels:

$$T(x,y,p,t)-T_n(p)=\sum_{i=1}^{s}\tau_i(p)\{H_i(x,y,t)-H_{ni}(p)\}+e(x,y,p,t) \tag{1}$$

$e(x,y,p,t)$ is the residual at time t, or the unexplained part of $T(x,y,p,t)$.

$T_n(p)$ is the normal temperature at the level p, and $H_{ni}(p)$ is the normal height of the i'th isobaric level of reference. In case the thickness H_j-H_i is the best estimate of the temperature, we would find that $-\tau_i(p)$ is equal to $\tau_j(p)$.

The hydrostatic equation may be written as follows

$$\frac{\partial z}{\partial p}=-\frac{RT}{gp} \tag{2}$$

where z from now on denotes the height of isobaric levels. R is the gas constant and g the acceleration of gravity. Multiplying equation (2) by the operator $\boldsymbol{k}x\nabla\equiv\boldsymbol{k}x\left(\boldsymbol{i}\frac{\partial}{\partial x}+\boldsymbol{j}\frac{\partial}{\partial y}\right)$, we derive this relation

$$\frac{\partial(\boldsymbol{k}x\nabla z)}{\partial p}=-\frac{R}{gp}\boldsymbol{k}x\nabla T\approx-\frac{R}{gp}\sum_{i=1}^{s}\tau_i(p)\boldsymbol{k}x\nabla H_i \tag{3}$$

using the empirical relation (1). Applying the geostrophic assumption we find

$$\frac{\partial\boldsymbol{v}}{\partial p}\approx-\frac{R}{gp}\sum_{i=1}^{s}\tau_i(p)\boldsymbol{v}_i\,, \tag{4}$$

which integrated with respect to pressure gives

$$\boldsymbol{v}(x,y,p,t)\approx\sum_{i=1}^{s}A_i(p)\boldsymbol{v}_i(x,y,t) \tag{5}$$

if the constant of integration is included in one of the $A_i(p)$'s. The functions $A_i(p)$ were also evaluated directly from actual wind soundings, but no significant differences were found.

The thermodynamic equation may be written as follows

$$\frac{\partial T}{\partial t}+v\cdot\nabla T+\omega\left(\frac{\partial T}{\partial p}-\frac{RT}{c_p p}\right)=\frac{1}{c_p}\frac{\delta Q}{\delta t}\equiv H \tag{6}$$

$\delta Q/\delta t$ is the heat supplied per unit of time, and ω is the time rate of change of p following the motion. When inserting the relations (5) and (1) into relation (6), and rearranging the terms, we notice that

$$\omega\approx\frac{\sum_i \tau_i\frac{\partial H_i}{\partial t}+\sum_{i,j}\tau_i v_{id}\cdot\nabla H_j+\sum_{i<j}(A_i\tau_j-A_j\tau_i)k\cdot\nabla H_i\times\nabla H_j-H}{\left(\frac{RT_n}{c_p p}-\frac{dT_n}{dp}\right)+\sum_i\left(\frac{R\tau_i}{c_p p}-\frac{d\tau_i}{dp}\right)(H_i-H_{ni})} \tag{7}$$

$v_{id}(x, y, t)$is the ageostrophic component of the wind, and $H_{ni}(p)$ is the mean height of the i'th isobaric level. The second term of the numerator is generally important. If

$$\lim_{p\to 0}\left(\frac{RT_n}{c_p p}-\frac{dT_n}{dp}\right)>0\,,\quad \lim_{p\to 0}\tau_i(p)\infty p^{1+\varepsilon^2}\,,\quad \lim_{p\to 0}H=0\,, \tag{8}$$

the dynamic boundary condition $\lim_{p\to 0}\omega=0$ is satisfied. The denominator of relation (7) is proportional to the static stability. Before we present some observational evidence in support of our analysis, we shall introduce the following definitions:

$$\begin{aligned}\Gamma(x,y,p,t)&=\left(\frac{RT_n}{c_p p}-\frac{dT_n}{dp}\right)+\sum_{i=1}^{s}\left(\frac{R\tau_i}{c_p p}-\frac{d\tau_i}{dp}\right)(H_i-H_{ni})\\&\equiv\Gamma_n(p)+\sum_{i=1}^{s}B_i(p)\{H_i(x,y,t)-H_{ni}(p)\}\end{aligned} \tag{9}$$

$\Gamma_n(p)=(RT_n/c_p p-dT_n/dp)$ is always positive, and becomes very large in the stratosphere. In the troposphere, however, the other terms may become important in regions where the height deviate much from its normal value.

6. The case s = 1, one layer models. As H_{300} is consistently the best of levels when specifying the tropospheric conditions, we shall now present some results for the case $H_1=H_{300}$. If we put all monthly estimates of $\tau_1(p)$ at 600 mb, 500 mb and 400 mb together, we can construct Table 3. We find indications of some annual and geographical variations. Figure 9 gives the vertical distribution of $\tau_1(p)$.

Table 3. $\tau_1(p)$ in °F/100 ft at the levels of 600 mb, 500 mb and 400 mb.

Interval	Station			
	Lerwick	Downham Market	Jig Juliette	Mean
October—November	1.206	1.233	1.287	1.242
December—January	1.216	1.262	1.343	1.274
February—March	1.205	1.163	1.078	1.148
Mean	1.209	1.219	1.236	1.221

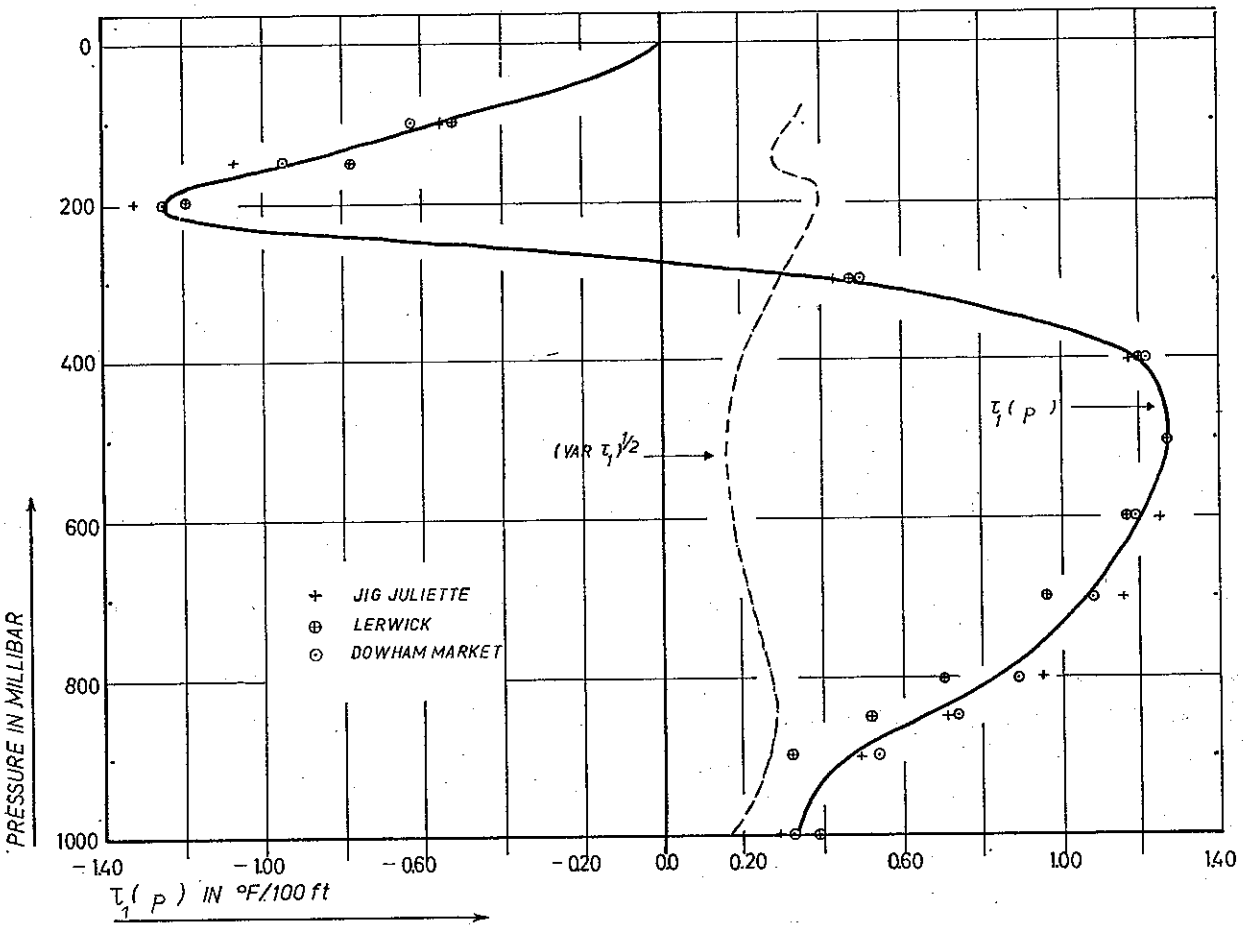

Fig. 9. $\tau_1(p)$ in °F/100 ft when $H_1=H_{300}$.

We may notice some geographical variations in the lower troposphere. Putting all 36 monthly estimates at each mb-level in one group, we can compute the variance at various levels. The curve for the standard deviation of $\tau_1(p)$ is drawn (broken curve) in Fig. 9. Remembering that both annual and geographical variations increase the variance, the broken curve indicate that the derived values of $\tau_1(p)$ should be fairly typical for most atmospheric circulations in the Eastern Atlantic region. We may also derive a frequency distribution of $\tau_1(p)$ by considering the 72 cases at 600 mb and 400 mb, as $\overline{\tau_1(400)}=\overline{\tau_2(600)}=1.20$ °F/100 ft. The distribution is fairly symmetric around the mean value, see Table 4. Another result which may be useful, is the following relation which holds for all levels from surface to 150 mb.

$$\overline{\tau_1(p)} \approx 1.01 \overline{r_{T(p)H}}^{z} \{\overline{\text{var}\, T(p)}\}^{\frac{1}{2}} \{\overline{\text{var}\, H_1}\}^{-\frac{1}{2}} \quad (10)$$

A bar followed by a z denotes that the average is derived from the z-transformed values.

Table 4. *Frequencies of $\tau_1(400)$ and $\tau_1(600)$ in °F/100 ft, when H_1 is height of 300 mb.*

Interval	0.50→ 0.89	0.90→ 0.99	1.00→ 1.09	1.10→ 1.19	1.20→ 1.29	1.30→ 1.39	1.40→ 1.49	1.50→ 1.59
Frequency	2	9	10	15	15	12	6	3

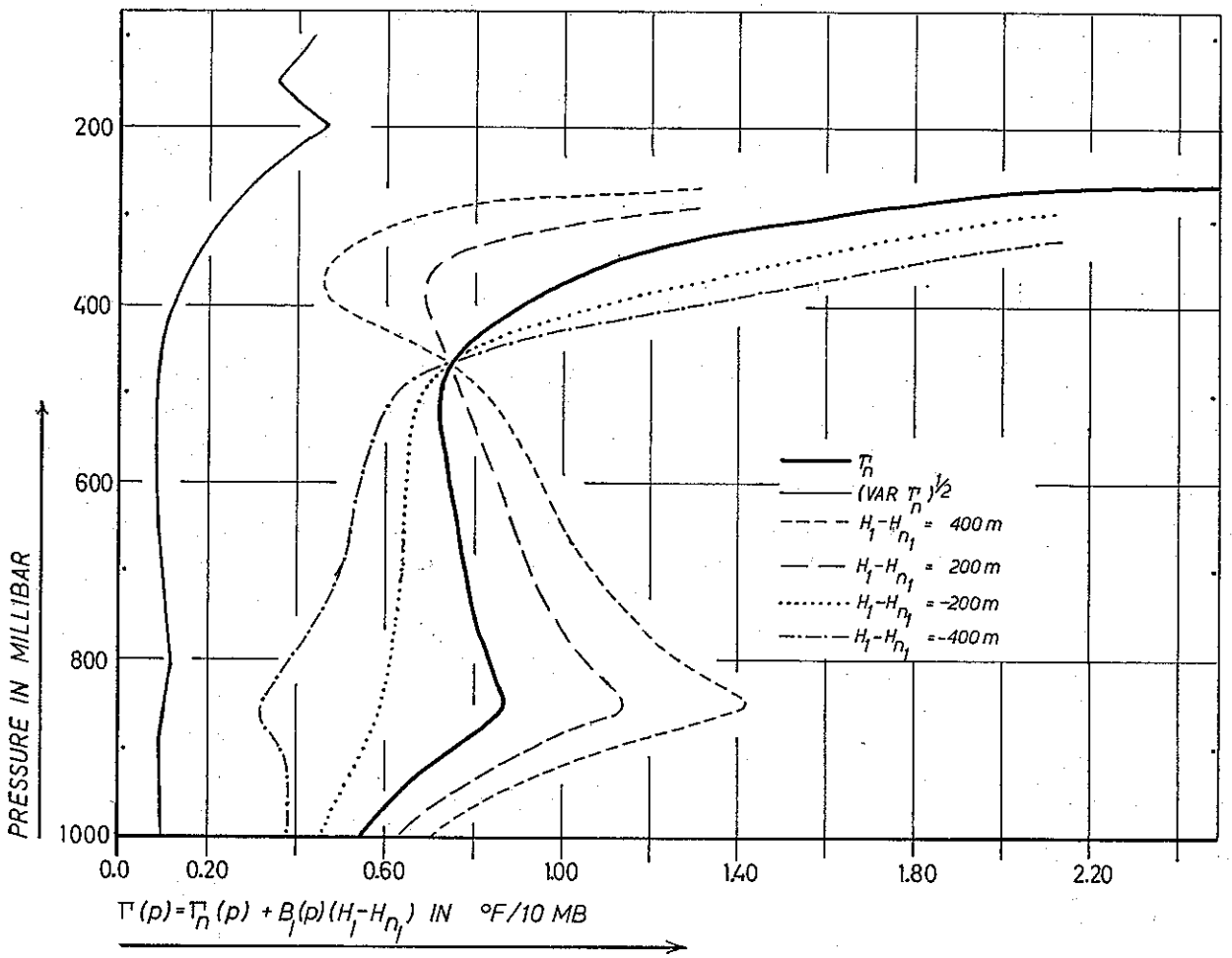

Fig. 10. $\Gamma(p)$ in °F/10 mb as a function of height anomaly.

We shall now proceed to the next step which consists of computing $\Gamma_n(p)$ and $B_1(p)$, which are both defined by equation (9). As $B_1(p)=\left(\frac{R\tau_1}{c_p p}-\frac{d\tau_1}{dp}\right)>0$ in most of the troposphere, this variable part of the static stability is negative in troughs (depressions) and positive in ridges (highs). The values of $\Gamma_n(p)$ are high in the stratosphere, see Table 5 where we have tabulated $\Gamma(x,y,p,t)=\Gamma_n(p)+B_1(p)\{H_1(x,y,t)-H_n(p)\}$ for height anomalies of 0 m, 200 m and 400 m. We have chosen these deviations, as the standard deviation of H_{300} is close to 200 m in the winter season. We notice that $\Gamma(p)$ is approximately proportional to p^{-1} when $p<200$ mb.

Table 5 reveals that $\Gamma(300)$ depends very much on the height anomaly, and turning now to Fig. 10 we learn that this is also the case for many levels in the troposphere. Most pronounced is the variability in the layer between 900 mb and 700 mb. But as a general conclusion we may say that the variation of $\Gamma(p)$ is almost of the same order as that of $\Gamma_n(p)$. In Fig. 10 we have also drawn the curve of $\{\mathrm{var}\Gamma_n(p)\}^{\frac{1}{2}}$ based on the monthly estimates, and we notice that this standard deviation is close to 0.10 °F/10 mb

Table 5. *$\Gamma(p)$ in °F/10 mb for levels above 300 mb.*

$H_1 - H_{n1}$	− 400 m	− 200 m	0 m	+ 200 m	+ 400 m
$\Gamma(300)$	2.49	2.04	1.58	1.13	0.67
$\Gamma(200)$	5.18	5.48	5.79	6.09	6.39
$\Gamma(150)$	6.66	6.99	7.32	7.66	7.99
$\Gamma(100)$	9.90	10.27	10.65	11.02	11.39
$\Gamma(50)$	19.3	19.7	20	20.3	20.7

in the troposphere. The model implements of the curves in Fig. 10 is best illustrated by relation (7). If we put $\Gamma(p) = \Gamma_n(p)$, which has been done in many models, the ω-values derived from equation (7) will, at the levels below 500 mb, have too high numerical values in highs and too low numerical values in lows.

The vertical wind distribution is given in Fig. 11. We have also computed the variance of $A_1(p)$. The variability seems to be rather high in the stratosphere.

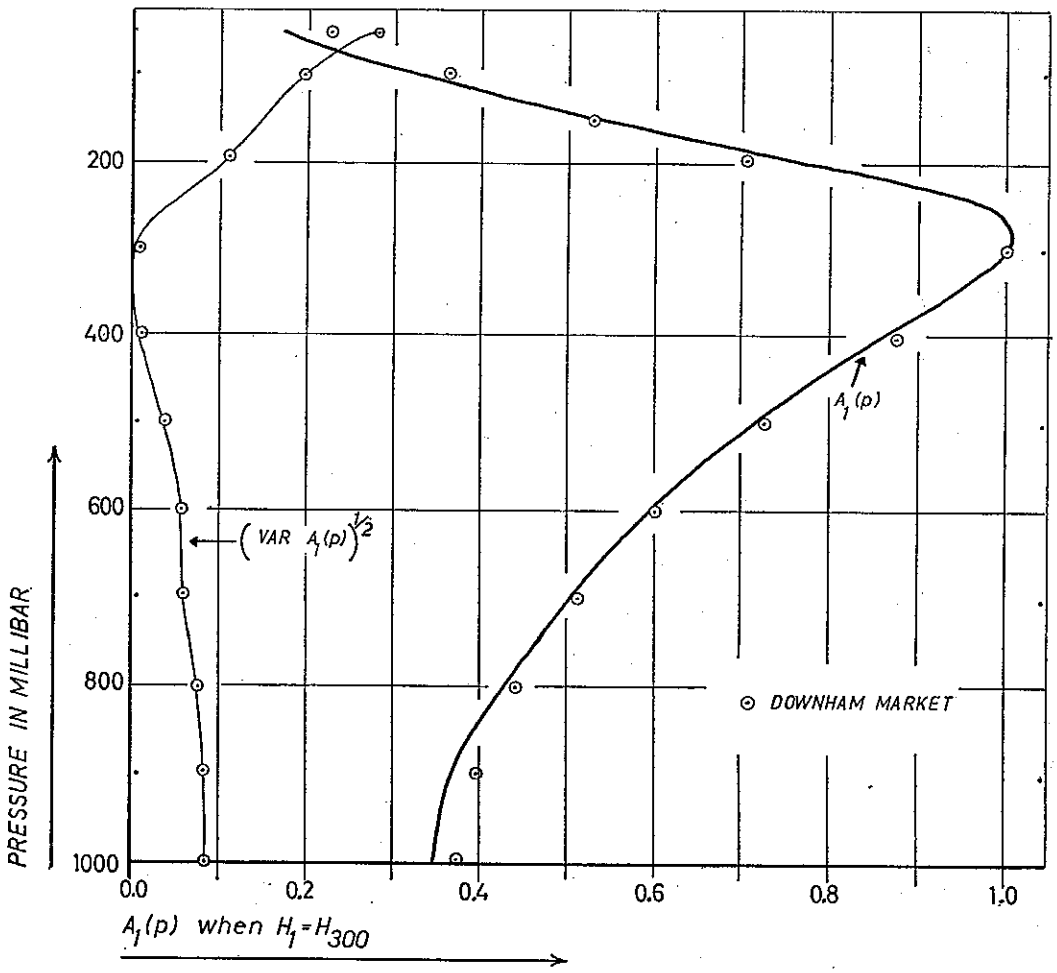

Fig. 11. $A_1(p)$ as a function of pressure, when $H_1 = H_{300}$.

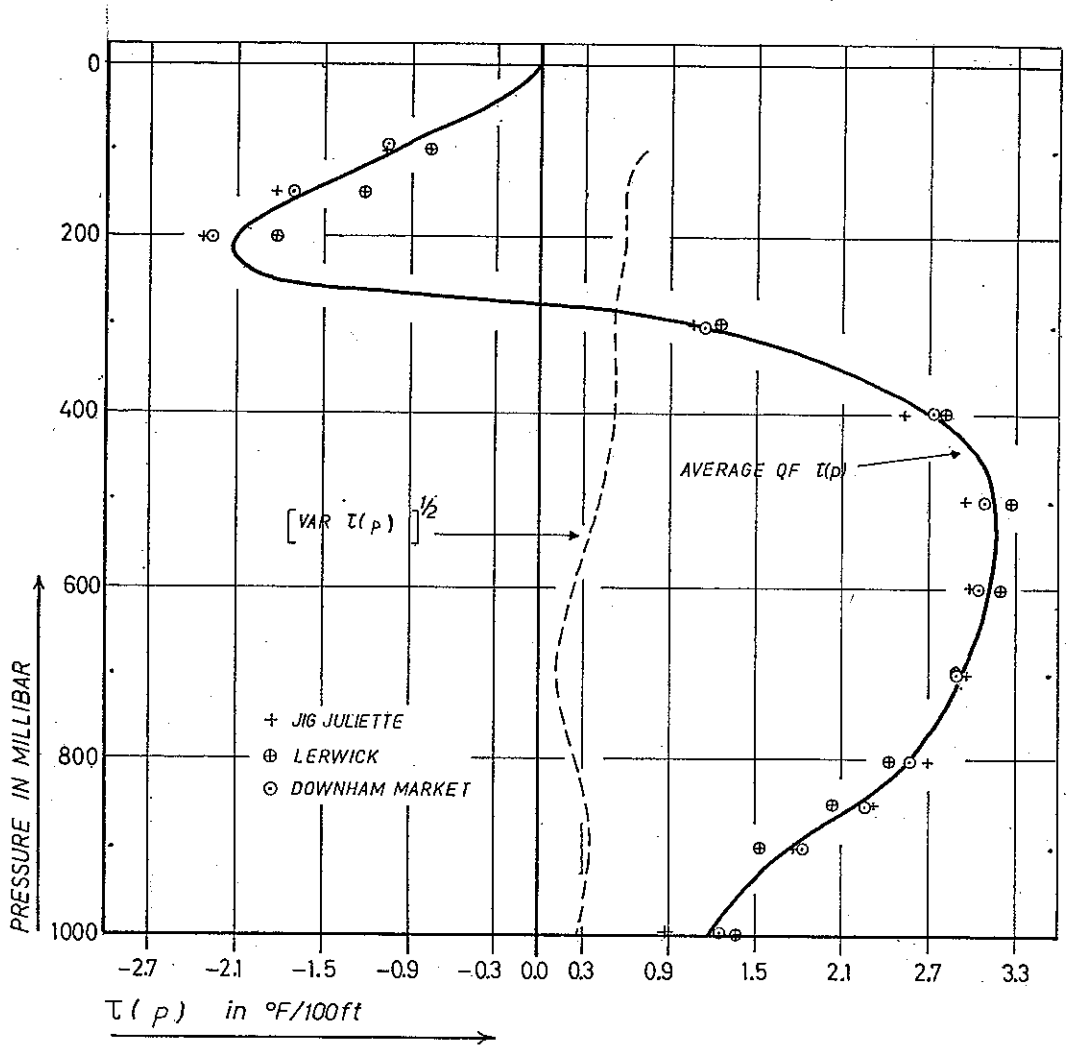

Fig. 12. $\tau_{h_{500}}(p)$ in °F/100 ft as a function of pressure.

7. Models where one thickness is used to describe the vertical wind and temperature distributions. In Fig. 6 we noticed that the thicknesses h_{500} and h_{300} would describe the tropospheric temperature distribution fairly well. As the geostrophic wind shear is proportional to the regression constants $\tau_{h_{500}}(p)$ and $\tau_{h_{300}}(p)$, these two functions are displayed in Fig. 12 and Fig. 13. We have also drawn the standard deviations of the regression constants as to demonstrate the joint effects of sampling, geographic variation and annual trend. The standard deviations are, as before, computed from the 36 individual monthly estimates at each pressure level. The low variability of $\tau_{h_{500}}(p)$ at the 700 mb level is noticeable. Likewise, $\tau_{h_{300}}(p)$ has a low, almost constant, standard deviation throughout the troposphere.

We may derive formulae analogues to relations (3) and (4), describing the thermal wind distribution,

$$\frac{\partial v(x, y, p, t)}{\partial p} \approx -\frac{R\tau_h(p)}{gp} v_T(x, y, t) \tag{11}$$

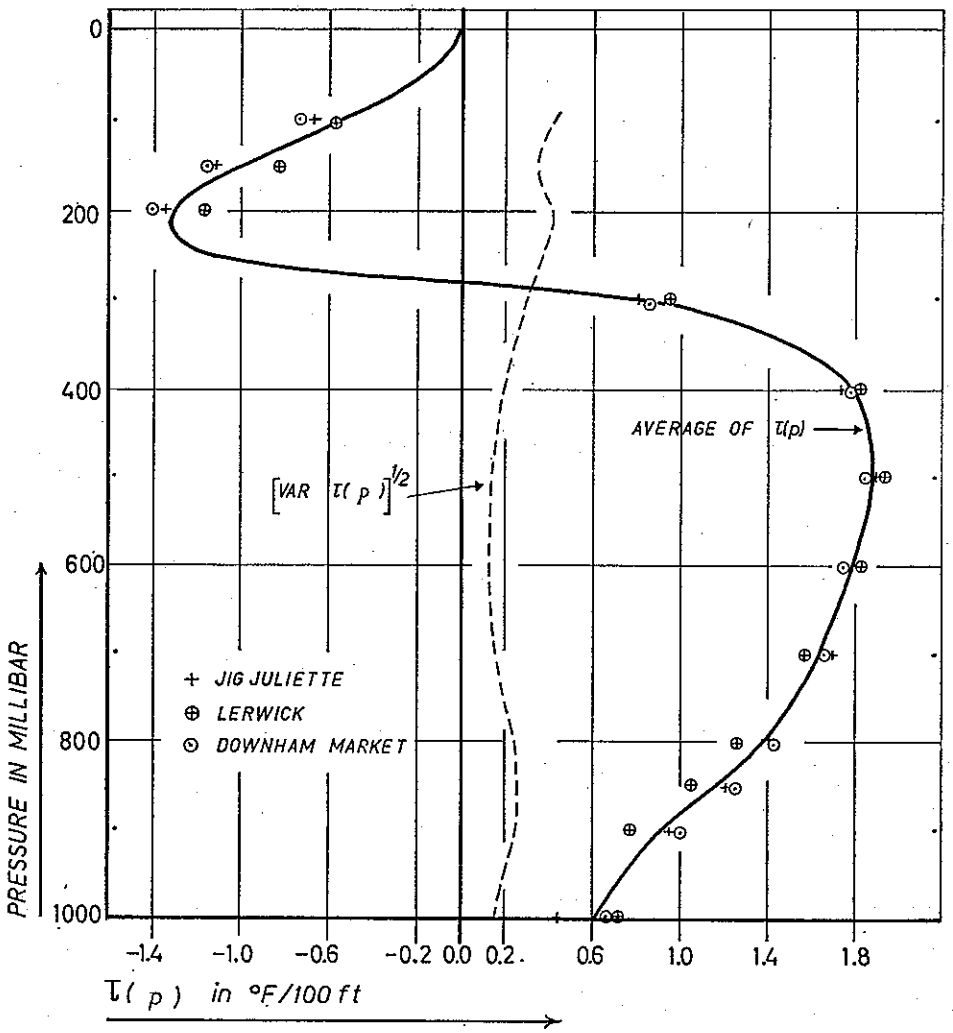

Fig. 13. $\tau_{h_{300}}(p)$ in °F/100 ft as a function of pressure.

where

$$v_T(x, y,)=\frac{g}{f}kx\nabla h(x, y, t) \tag{12}$$

Integration of (11) with respect to pressure gives, denoting pressure averages by a bar,

$$v(x, y, p, t)\approx v_1(x, y, t)+A^*(p)v_T(x, y, t)=\bar{v}(x, y, t)+A(p)v_T(x, y, t) \tag{13}$$

where $A^*(p_1)=0$ and $\overline{A(p)}=0$. We may also establish formulae similar to relations (6) through (9) replacing H_1 by h. Plotting $\Gamma(p)$ for this latter case, see Figs. 14 and 15, we notice no significant deviations from the curve derived for H_1, which was given in Fig. 10. The functions $A(p)$ are shown in Fig. 16 for the two thicknesses considered. We may notice that the two curves give $v=\bar{v}$ at pressure levels close to 550 mb and 100 mb.

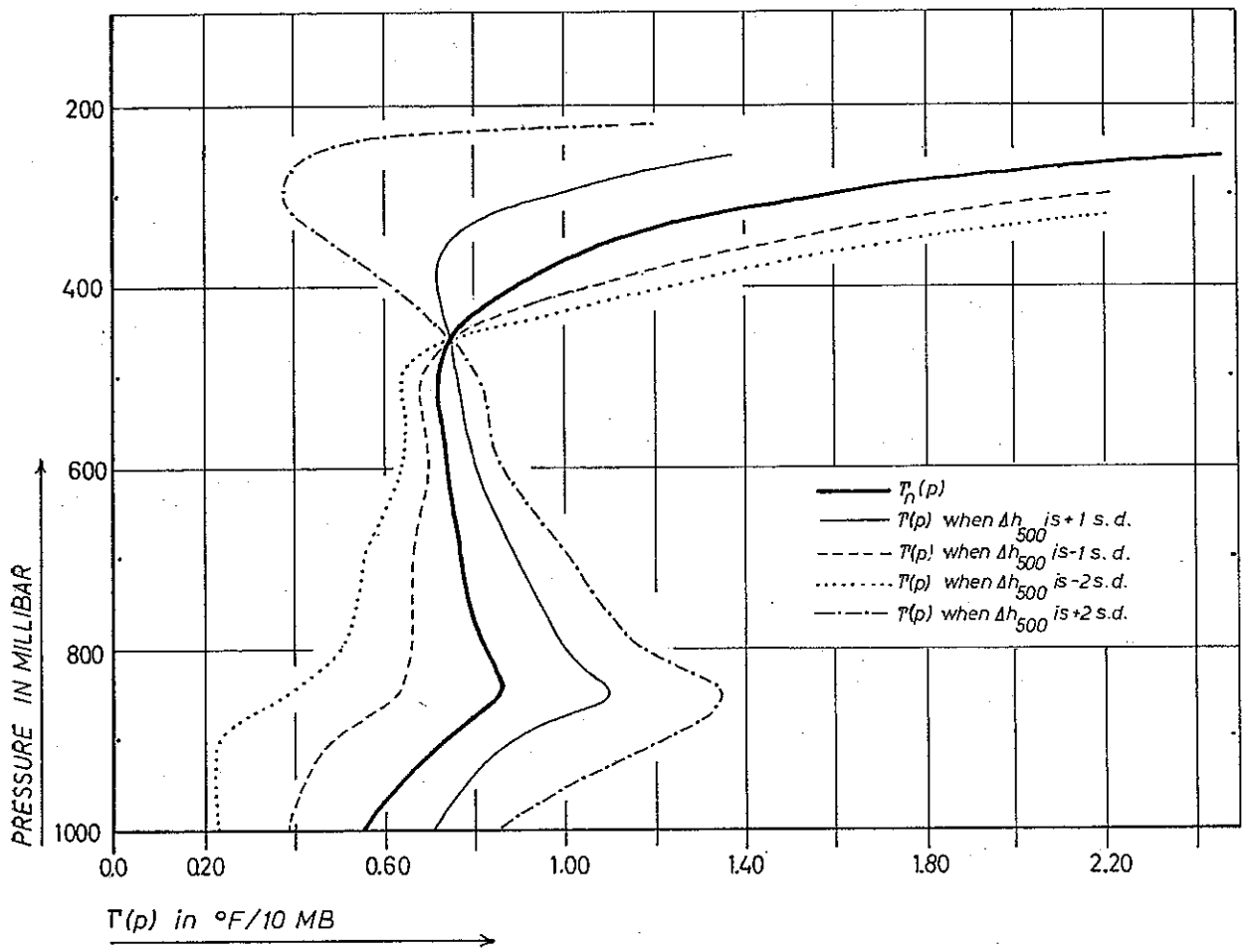

Fig. 14. $\Gamma(p)$ in °F/10 mb, using h_{500} as temperature parameter.

8. Some comments on the more general two level model. As shown in Fig. (6), we may empirically derive a two level model which formally has two degrees of freedom in the temperature field,

$$T(x,y,p,t)=T(p)+\tau_1(p)\{H_1(x,y,t)-H_{n1}(p)\}+\tau_2(p)\{H_2(x,y,t)-H_{n2}(p)\}+e(x,p,y,t) \quad (14)$$

We can also show that a level close to the tropopause, and another level, not too far from the surface, will generally minimize the pressure integral of the residual variances of equation (14). If we choose the heights of the levels 300 mb and 1000 mb as $H_1(x,y,t)$ and $H_2(x,y,t)$ respectively, we derive the curves of Fig. 17 for the period under consideration. Looking back to Fig. 9 we notice that the $\tau_1(p)$ curve is fairly similar to that of Fig. 17. $-\tau_2(p)$ is, as a rather crude approximation, equal to $\tau_1(p)$ through a significant part of the troposphere, suggesting that the thickness h_{300} is a fairly good temperature parameter in the troposphere. The stratospheric behaviour of $\tau_2(p)$ might also look interesting, but should not be taken too seriously. The reason for this is that if our curves

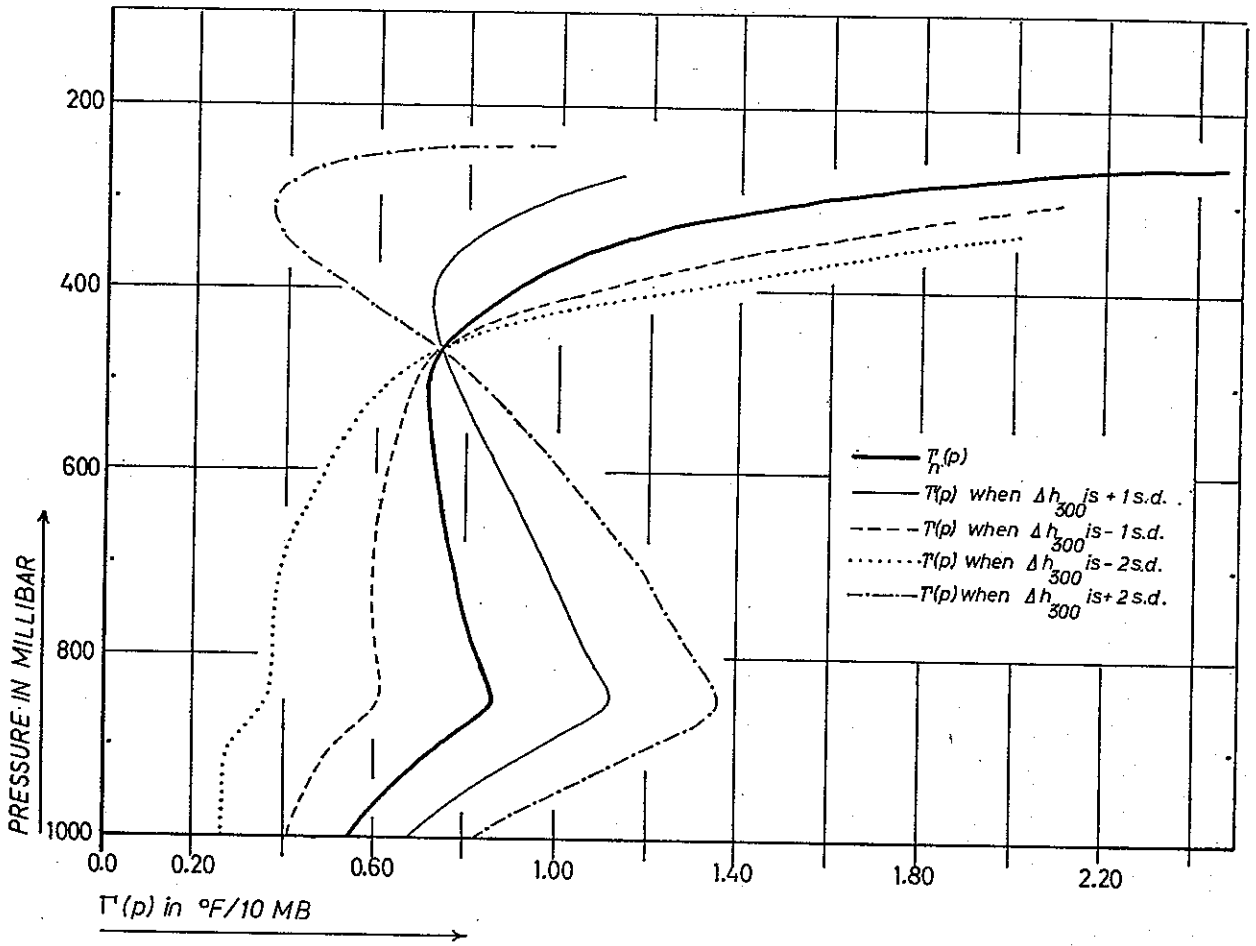

Fig. 15. $\Gamma(p)$ in °F/10 mb, using h_{300} as temperature parameter.

are derived by the least squares regression analysis, their shape may be strongly deformed because of "noise" effects. In this paper, as in most other synoptical investigations, we have to restrict ourselves to motions on scales larger than twice the distance between our gridpoints, or stations. Instrumental errors and transmission errors, and motions on scales less than those under consideration, may all give significant contributions to our matrix of covariance, from which most of our statistical estimates are derived. As some of these "noise" effects may create quite a confusion in our analysis, we shall try to give a very short summary in this paper. For a more complete discussion, we may refer to papers by A. ELIASSEN (1954), by NORDØ (1958), and by TREFALL and NORDØ (1959).

We shall now try to demonstrate that almost any empirically derived relation will contain *systematic* distortions, which sometimes may rule out any chance of detecting the real physical relationship being present in our data. The larger our number of parameters becomes, the more likely a failure becomes. We will denote the values on scales under consideration as "true" values, and mark these values by an apostrophe.

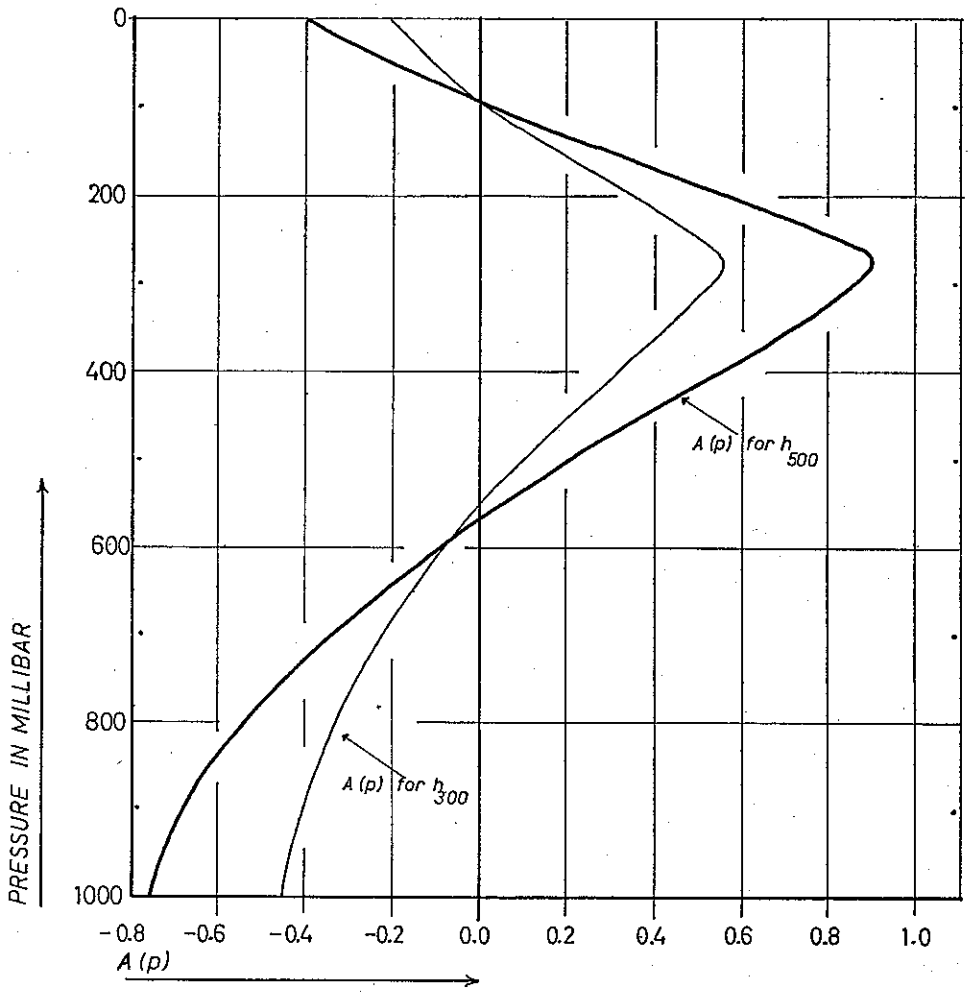

Fig. 16. Vertical wind distributions when tropopsheric thicknesses are used as shear parameters.

Let us further on denote the total "noise" effect of x_i by δ_i, and the "noise" effect of y (our independent variable) by δ. Suppose also that all mean values are zero, and that

$$\overline{x_i'\delta}=\overline{x_i'\delta_i}=\overline{\delta\delta_i}=\overline{y'\delta_i}=\overline{y'\delta}=0\,, \tag{15a}$$

and

$$\overline{x_i'\delta_j}=\overline{\delta_i\delta_j}=0\,, \tag{15b}$$

for $i\neq j$.

Let us just inspect the case $i=1$. Then we find that

$$|b_1|=\frac{\overline{|x_1y|}}{\overline{x_1^2}}=\frac{\overline{|x_1'y'|}}{\overline{x_1'^2}+\overline{\delta_1^2}}<|b_1'|\,,\quad r<r_1'\,,\quad \overline{e^2}>\overline{e'^2}\,, \tag{16}$$

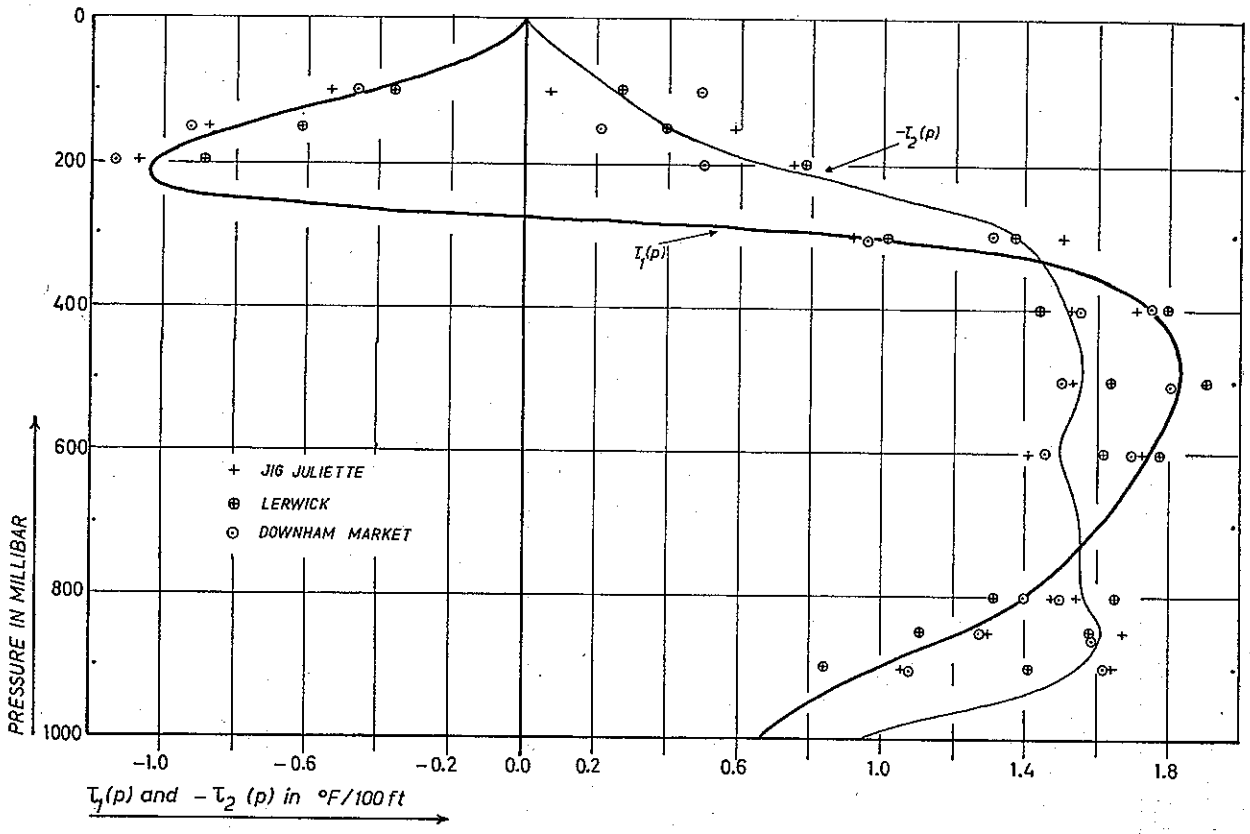

Fig. 17. $\tau_1(p)$ and $\tau_2(p)$ in °F/100 ft when $H_1=H_{300}$ and $H_2=H_{1000}$.

the marked quantities being the "true" ones, b the coefficient of regression, r the coefficient of correlation, and $\overline{e^2}$ the residual variance. If we increase the number of dependent variables to, say 10, the empirical constants b_i will deviate much from their true values, even for quite moderate values of the error variances. In the general case the errors may be correlated to the "true" values, and relation (15) is not fulfilled any longer. TREFALL and NORDØ (1959) have considered such a case where the uncorrected empirical relations did not agree with the theoretical estimates, but where the agreement was satisfactory after the corrections were made. Such systematic effects due to "noise" scales etc. cannot, of course, be eliminated by stratification of the data or by similar methods. We ought therefore to put more efforts in the study of, and the estimation of, various "error" distributions. Some observational schemes have been designed especially for this purpose, see e.g. NORDØ (1958). If we have some estimates of these error covariances, we may correct the original matrix of covariance, compare e.g. TREFALL and NORDØ (1959). But we shall always keep in mind that our corrections may just remove some first order effects caused by the "noise" field. Statistical estimates based on solutions of a matrix of order 10 or more, may still be strongly biased, and should be considered with quite a lot of scepticism. Some matrices based on surface pressure data may, however, give reliable results because of the small error variances.

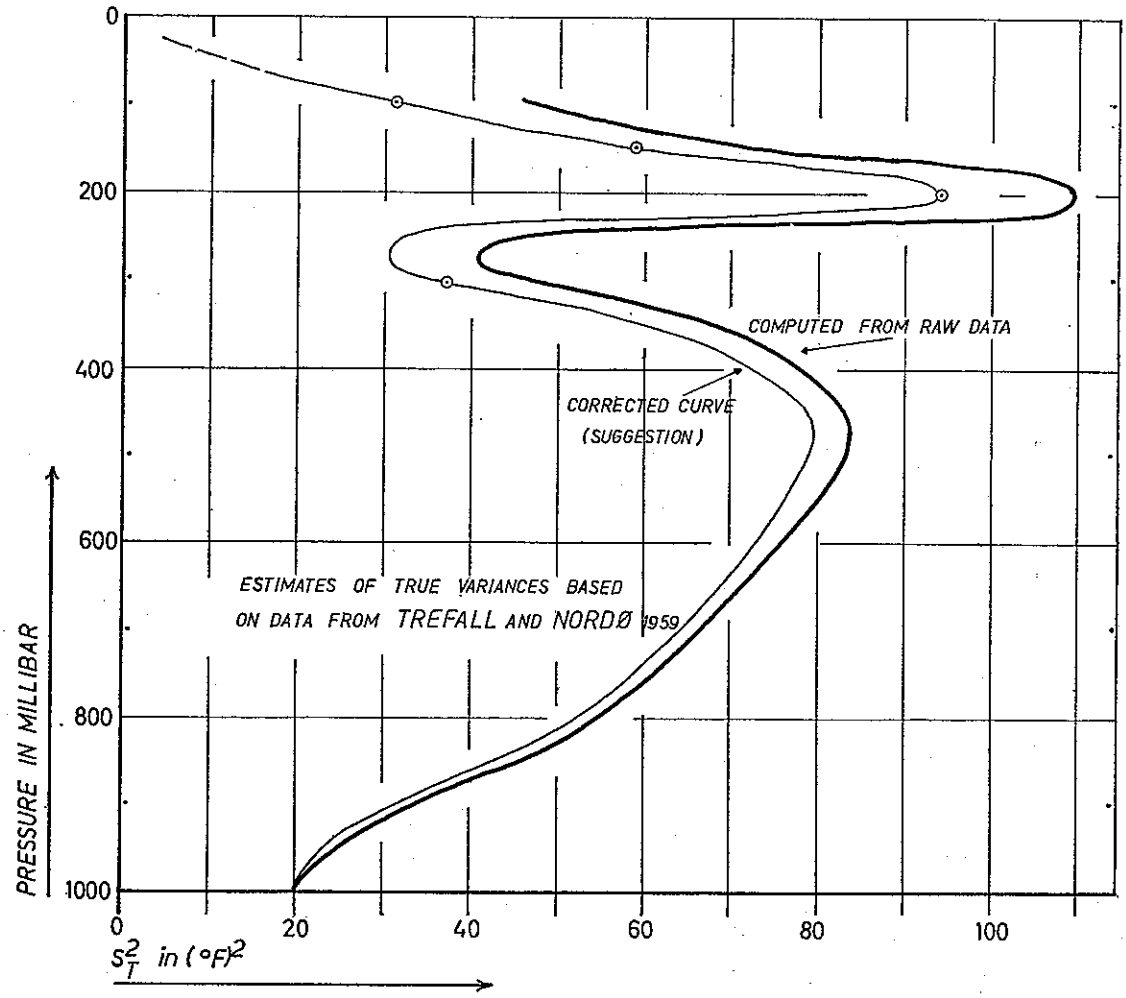

Fig. 18. Suggestive corrections of the temperature variances.

We shall now try to correct the values of $\tau_1(p)$ and $\tau_2(p)$ at levels at and above 300 mb. In Fig. 18 we have suggested a "true" curve for the variation of temperature, using the results from the papers referred to above.

Using the corrections, and smoothing the results somewhat, we find the curves given in Fig. 19. Except for the surface layer, $\tau_2(p)$ may be considered as almost constant in the troposphere, and close to zero in the stratosphere. The amplitude of $\tau_1(p)$ has increased in the stratosphere.

Applying the operator $gf^{-1}kx\nabla$ on relation (14) and integrating with respect to p (using the corrected values), we derive

$$v(x,y,p,t)\approx A_1(p)v_1(x,y,t)+A_2(p)v_2(x,y,t) \tag{17}$$

The constant of integration was included in $A_2(p)$ to give $A_2(1000)=1$. Figure 20 gives then the derived distributions of $A_1(p)$ and $A_2(p)$. We may notice that $A_1(1000)=A_2(300)=0$ and that $A_1(300)=A_2(1000)=1$, and that these equations were almost exactly

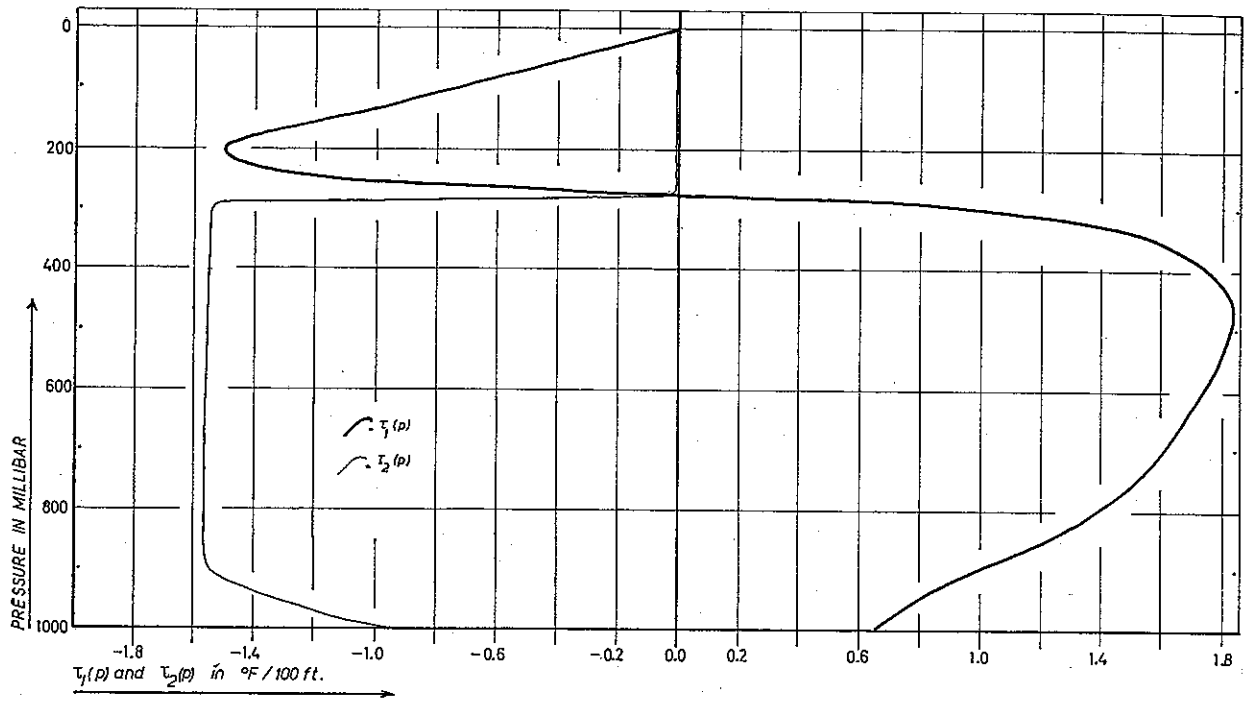

Fig. 19. "Corrected" values of $\tau_1(p)$ and $\tau_2(p)$ in °F/100 ft.

fulfilled *before* correcting the 300 mb values of $\tau_1(p)$ and $\tau_2(p)$. The curves of $A_1(p)$ and $A_2(p)$ are crossing each other close to 535 mb, $A_1(535)=A_2(535)=0.49$.

Since our values of $A_1(p)$ and $A_2(p)$ show reasonable variations at least within the troposphere, the author feels that relations (17) and (14) may be very useful in the balanced models. The advantage of our approach compared to a classical one, is the improved estimation of the pressure derivatives because of our optimal approach.

The function $\Gamma(x, y, p, t)$ is given by the following relation

$$\Gamma(x,y,p,t)=\Gamma_n(p)+B_1(p)\{H_1(x,y,t)-H_{n1}(p)\}+B_2(p)\{H_2(x,y,t)-H_{n2}(p)\} \qquad (18)$$

Relation (18) may describe a variety of static stability distributions. Some extreme cases are drawn in Fig. 21. We may notice that the surface layer may locally become staticly unstable. When H_1 is high, the static stability may be low up to the 250 mb level, but on the other hand very high near the surface.

9. Some ways of extending the preceding analysis to geostrophic multilayer models, as well as to primitive equation models. We did extend our analysis to some optimal 3-level models, and in principle it is easy nowadays to introduce still more layers. But the preceding error analysis suggests strongly that we should not extend our analysis until more is known about the energy on various "noise" scales. For operational use we have to establish the functions $A_i(p)$, $\tau_i(p)$, $H_{ni}(p)$, $T_n(p)$ for each season, and for 20—50 stations suitably located over the whole hemisphere. These empirical

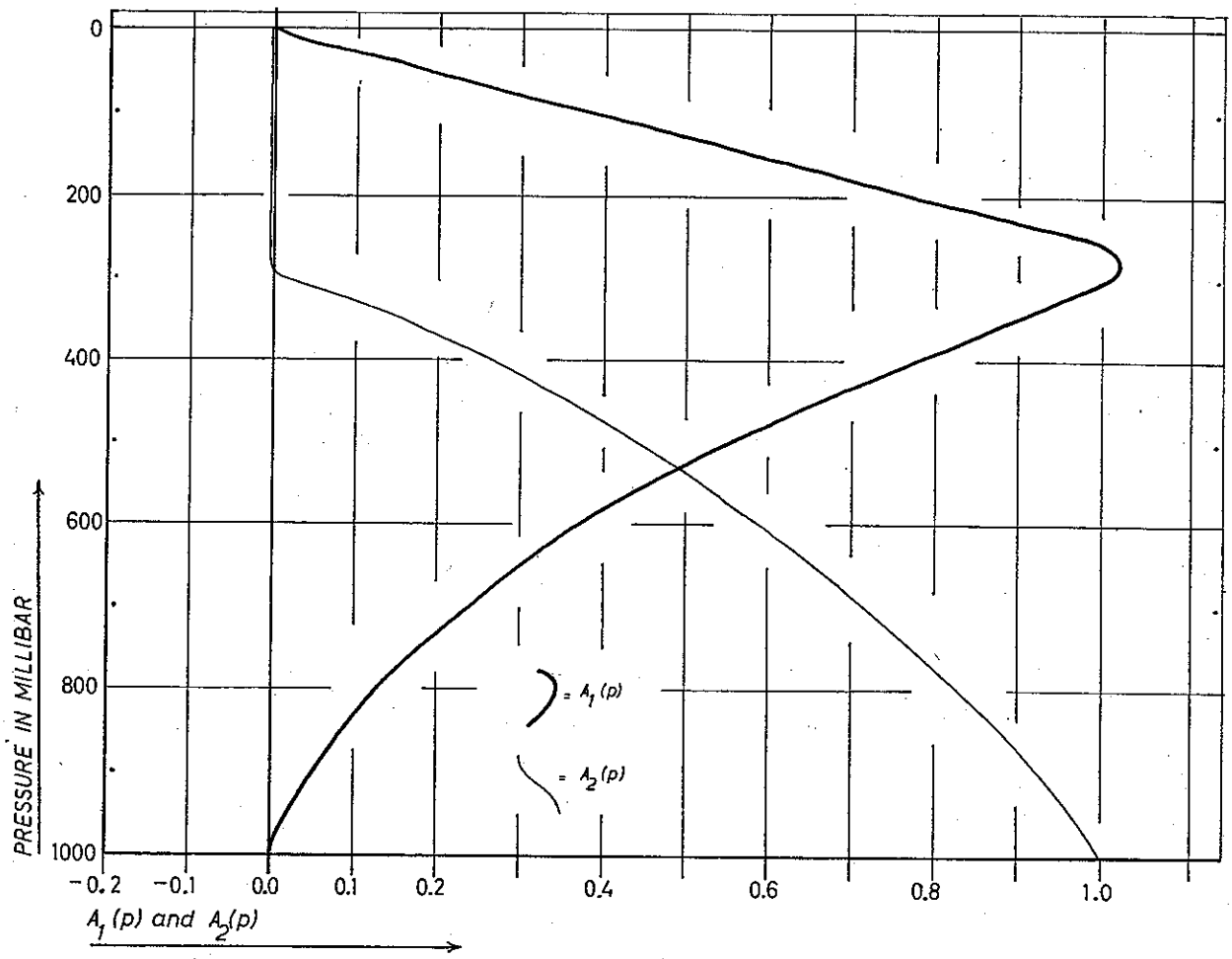

Fig. 20. $A_1(p)$ and $A_2(p)$ when $H_1=H_{300}$ and $H_2=H_{1000}$..

functions will now appear to become variable in space. But the spatial differentiations of the empirical functions should be rather small, and might only be considered in connection with extended time integrations, or with integration of the very longest waves.

The preceding procedure might be useful in specifying the tropopause height and wind as functions of the conditions at, say 100 mb and 300 mb. Furthermore, the complicated processes going on in the surface layer might also be described by such empirical relationships.

Relation (5) was also established directly from wind data for both of the horizontal wind components. Some anisotropy was found, but as a first approximation the results are similar to those established for the geostrophic part of the wind. This finding might have been anticipated as the ageostrophic component of the wind is relatively small. Special diagnostic equations may resolve this component from the overall wind, before establishing the optimal regression equations using height fields and geostrophic winds as predictors. Such a procedure requires reliable data and extensive computation facilities, and an extensive investigation was almost impossible 10 years ago.

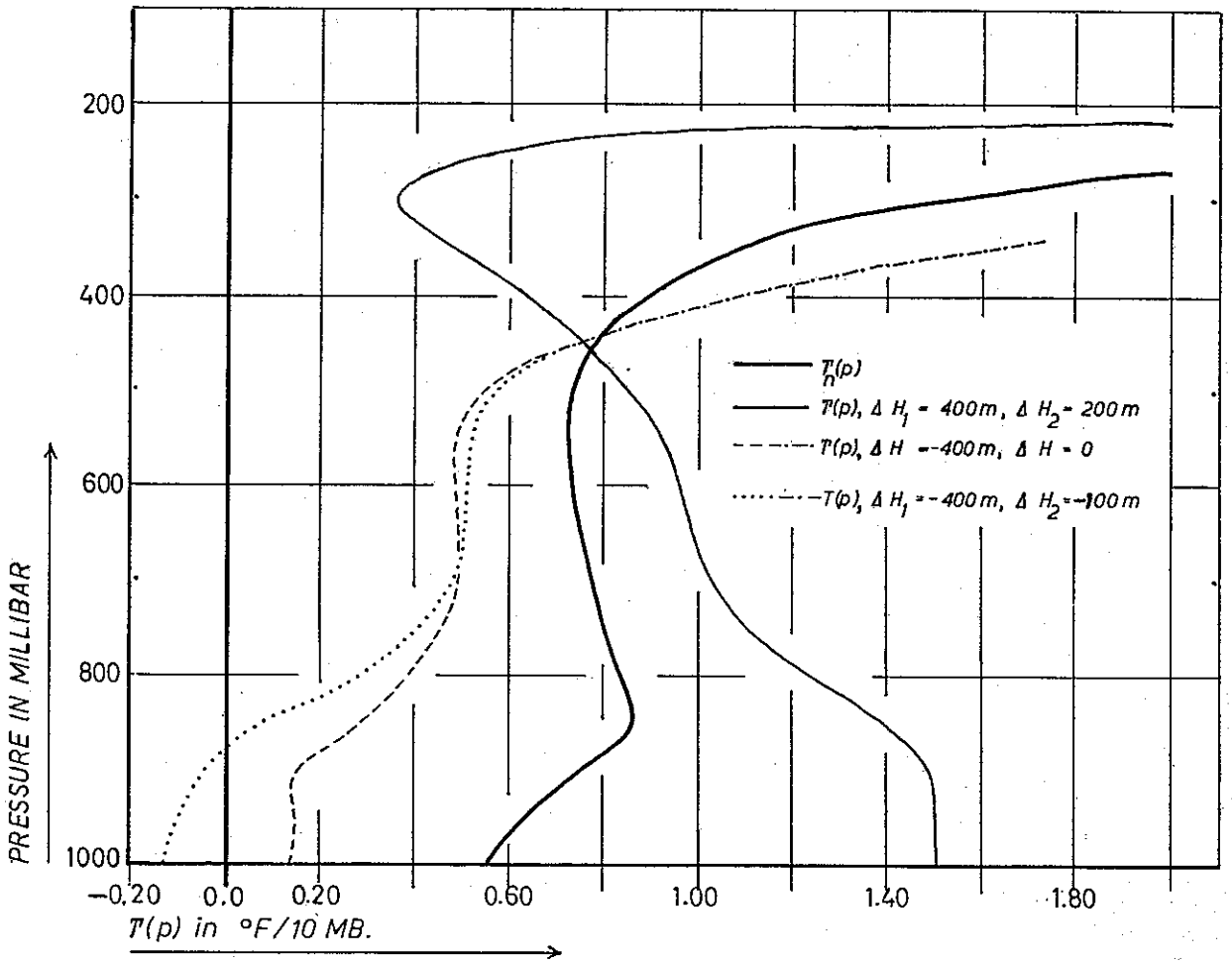

Fig. 21. $\Gamma(p)$ in °F/10 mb as a function of H_{800} and H_{1000}.

Sometimes it may be convenient to transform the derived relations to a set of orthogonal polynomials, for mathematical reasons. But as the theory of linear transformations is well known, and OBUKHOV (1960) and HOLMSTRÖM (1963, 1964) have carried out similar studies, the various transformations will not be discussed in this paper.

10. Concluding remarks. We feel that further empirical studies of the atmospheric structure will yield more significant results than those derived so far. The reason for this statement being partly the improved data series collected during the past ten years, and partly the increased possibility of using computers to derive the very most optimal relationships which exist, see e.g. NORDØ (1960). Having established such relationships, we may very well derive models with a vertical (possibly also a horizontal) resolution which equals that of much higher order model. In this way we may be able to perform many more numerical experiments, as the computer capacity and speed seem always to be some of the main barriers to further exploitation of the equations of motion.

Acknowledgement. We are very indebted to Dr. H. Solberg, who obtained the funds for the initial study. We are also thankful to Dr. E. N. Lorenz for his interest during our stay at Massachusetts Institute of Technology.

REFERENCES

CHARNEY, J. G., and N. A. PHILLIPS, 1953: Numerical integration of the quasi-geostrophic equations of motion for baroclinic flows. *J. of Meteor.* **10**, 71—99.

ELIASSEN, A., 1952: Simplified dynamic models of the atmosphere, designed for the purpose of numerical weather prediction. *Tellus*, **4**, 145—156.

— 1954: Provisional report on calculation of spatial covariance and autocorrelation of the pressure field. *Institute for Weather and Climate Research, The Norwegian Academy of Science and Letters, Report No. 5.*

FJØRTOFT, R., (1962): A numerical method of solving certain partial differential equations of second order. *Geophysica Norvegica*, **24**, No. 7, 229—239.

HOLMSTRÖM, I., 1963: On a method for parametric representation of the scale of the atmosphere. *Tellus*, **15**, 127—149.

— 1964: On the vertical structure of the atmosphere. *Tellus*, **16**, 288—308.

NORDØ, J., 1958: On linear regression analysis for data with observational errors. *The Norwegian Meteorological Institute. Sci. Report* No. 3.

— 1960: Significance of regression equations derived from serially correlated data, and a procedure of selecting optimal predictors. *The Norwegian Meteorological Institute, Sci. Report* No. 8, 15—18.

OBUKHOV, A. M., 1960: The statistically orthogonal expansions of empirical functions. *Izv. Geophys. Ser.* 1960, 432—439.

SMAGORINSKY, J. et al, 1965: Personal communication.

TREFALL, H., and J. NORDØ, 1959: On systematic errors in the least squares regression analysis, with application to the atmospheric effects on cosmic radiation. *Tellus*, **11**, 467—477.

WMO, 1965: Fourth report on the advancement of atmospheric sciences and their application in the light of developments in outer space. *Secretariat of the World Meteorological Organization*, Geneva, Switzerland.

Avhandlinger som ønskes opptatt i «Geofysiske Publikasjoner», må fremlegges i Videnskaps-Akademiet av et sakkyndig medlem.

Vol. XXI.

No. 1. A. Omholt: Studies on the excitation of aurora borealis II. The forbidden oxygen lines. 1959.
» 2. Tor Hagfors: Investigation of the scattering of radio waves at metric wavelengths in the lower ionosphere. 1959.
» 3. Håkon Mosby: Deep water in the Norwegian Sea. 1959.
» 4. Søren H. H. Larsen: On the scattering of ultraviolet solar radiation in the atmosphere with the ozone absorption considered. 1959.
» 5. Søren H. H. Larsen: Measurements of amospheric ozone at Spitsbergen (78°N) and Tromsø (70°N) during the winter season. 1959.
» 6. Enok Palm and Arne Foldvik: Contribution to the theory of two-dimensional montain waves 1960.
» 7. Kaare Pedersen and Marius Todsen: Some measurements of the micro-structure of fog and stratus-clouds in the Oslo area. 1960.
» 8. Kaare Pedersen: An experiment in numerical prediction of the 500 mb wind field. 1960.
» 9. Eigil Hesstvedt: On the physics of mother of pearl clouds. 1960.

Vol. XXII.

No. 1. L. Harang and K. Malmjord: Drift measurements of the E-layer at Kjeller and Tromsø during the international geophysical year 1957—58. 1960.
» 2. Leiv Harang and Anders Omholt: Luminosity curves of high aurorae. 1960.
» 3. Arnt Eliassen and Enok Palm: On the transfer of energy in stationary mountain waves. 1961.
» 4. Yngvar Gotaas: Mother of pearl clouds over Southern Norway, February 21, 1959. 1961.
» 5. H. Økland: An experiment in numeral integration of the barotropic equation by a quasi-Lagrangian method. 1962.
» 6. L. Vegard: Auroral investigations during the winter seasons 1957/58—1959/60 and their bearing on solar terrestrial relationships. 1961.
» 7. Gunnvald Bøyum: A study of evaporation and heat exchange between the sea surface and the atmosphere. 1962.

Vol. XXIII.

No. 1. Bernt Mæhlum: The sporadic E auroral zone. 1962.
» 2. Bernt Mæhlum: Small scale structure and drift in the sporadic E layer as observed in the auroral zone. 1962.
» 3. L. Harang and K. Malmjord: Determination of drift movements of the ionosphere at high latitudes from radio star scintillations. 1962.
» 4. Eyvind Riis: The stability of Couette-flow in non-stratified and stratified viscous fluids. 1962.
» 5. E. Frogner: Temperature changes on a large scale in the arctic winter stratosphere and their probable effects on the tropospheric circulation. 1962.
» 6. Odd H. Sælen: Studies in the Norwegian Atlantic Current. Part II: Investigations during the years 1954—59 in an area west of Stad. 1963.

Vol. XXIV.

In memory of Vilhelm Bjerknes on the 100th anniversary of his birth. 1962.

Vol. XXV.

No. 1. Kaare Pedersen: On the quantitative precipitation forecasting with a quasi-geostrophic model. 1963.
» 2. Peter Thrane: Perturbations in a baroclinic model atmosphere. 1963.
» 3. Eigil Hesstvedt: On the water vapor content in the high atmosphere. 1964.
» 4. Torbjørn Ellingsen: On periodic motions of an ideal fluid with an elastic boundary. 1964.
» 5. Jonas Ekman Fjeldstad: Internal waves of tidal origin. 1964.
» 6. A. Eftestøl and A. Omholt: Studies on the excitation of N_2 and N_2^+ bands in aurora. 1965.

Vol. XXVI.

No. 1. Eigil Hesstvedt: Some characteristics of the oxygen-hydrogen atmosphere. 1965.
» 2. William Blumen: A random model of momentum flux by mountain waves. 1965.
» 3. K. M. Storetvedt: Remanent magnetization of some dolerite intrusions in the Egersund Area, Southern Norway. 1966.
» 4. Martin Mork: The generation of surface waves by wind and their propagation from a storm area. 1966.

A.s John Griegs Boktrykkeri